Geophys. J. Int. (2004) **158,** 827–848 doi: 10.1111/j.1365-246X.2004.02363.x

3-D density model of the crust of southern and central Finland obtained from joint interpretation of the SVEKALAPKO crustal *P*-wave velocity models and gravity data

E. Kozlovskaya,[1] S. Elo,[3] S.-E. Hjelt,[1] J. Yliniemi,[2] M. Pirttijärvi[1,3] and SVEKALAPKO Seismic Tomography Working Group

[1] *Department of Geophysics, Oulu University,* PO Box 3000, FIN-90014, *Finland. E-mail: elena.kozlovskaya@oulu.fi*
[2] *Sodankylä Geophysical Observatory/Oulu Unit, University of Oulu, Oulu University,* FIN-90014, *Finland*
[3] *Geological Survey of Finland,* PO Box 96, *Espoo* FIN-02151, *Finland*

Accepted 2004 May 18. Received 2004 May 12; in original form 2003 March 18

SUMMARY

The paper presents a three-dimensional (3-D) density model of the crust of southern and central Finland. The large SVEKALAPKO seismic array experiment was carried out in this area during 1998–1999. One of the intermediate objectives of the experiment was compilation of a 3-D *P*-wave velocity model (V_p model) of the crust to provide crustal corrections for teleseismic *P*-wave traveltimes. The model was constructed from the results of previous controlled-source seismic (CSS) experiments in the area and was composed of two main crustal layers, an upper crust and a high-velocity lower crust with $V_p > 7.0$ km s^{-1}. The thickness of the crust in the model varies from 64 to 38 km and includes three pronounced troughs. We used this model and the results of petrophysical studies of bedrock density in Finland as *a priori* information to construct a 3-D density model of the crust in the SVEKALAPKO area. The initial results of gravity modelling demonstrated, however, that the model lacks information about lateral velocity variations in the upper and middle crust. To improve the fit of the model to the observed Bouguer anomaly, the model was corrected by introducing two additional layers, called the lower crust and the middle crust, with $6.8 < Vp < 7.0$ km s^{-1} and $6.4 < Vp < 6.8$ km s^{-1}, respectively. The depth to the upper boundaries of these layers was retrieved from the results of previous seismic profiles in the area and the values of density and velocity in the upper crust were constrained using the information on bedrock densities in Finland, the Bouguer anomaly and new data about the velocity distribution within the upper crust obtained from local event studies of the SVEKALAPKO seismic experiment. The corrected model was used as a starting model for inversion of the observed Bouguer anomaly. The resulting 3-D density model agrees well with the observed Bouguer anomaly and explains the sources of large-scale Bouguer anomalies in the region. The model demonstrates that there is no correlation between the observed Bouguer anomaly and Moho depth. Rather, the Moho depressions in the region mark the boundaries of crustal blocks with different types of density distribution and are associated with the presence of additional compensating masses within the crust. The high-velocity lower crust of density $3.1–3.25 \times 10^3$ kg m^{-3} does not completely compensate the Moho depressions and the compensation is mostly a result of the presence of additional dense material in the upper and middle crust. Thus, the Moho depressions in central and southern Finland are fully compensated, or even overcompensated. On the other hand, the Moho depression in the area of the Gulf of Bothnia is compensated only in its southern part, resulting in a regional-scale minimum of the Bouguer anomaly in the northern part of the depression. The varying degree of compensation may result from variation in the origin and age of the present-day Moho boundary in the region.

Key words: 3-D gravity modelling, density–velocity relationships, Fennoscandian Shield, gravity inversion.

1 INTRODUCTION

SVEKALAPKO (Svecofennian–Karelia–Lapland–Kola) (Hjelt *et al.* 1996) was one of the key projects of the EUROPROBE multidisciplinary geoscientific program concerned with the continental origin and evolution. The program was supported by the European Science Foundation (ESF) from 1992 to 2001. The main objectives of the project were to determine the geometry, thickness and age of the lithosphere and the disposition of major lithosphere structures in the Baltic Shield and to define the crustal evolutionary history along a transect through three major crustal segments: two contrasting Palaeoproterozoic orogens, Lapland–Kola and Svecofennian and the intervening Karelian craton (Fig. 1, inset; Hjelt *et al.* 1996).

The main goal of all the geophysical studies in the SVEKALAPKO multidisciplinary project was to investigate the structure of the lithosphere–asthenosphere boundary and the structures within the lithosphere of the central part of the Fennoscandian Shield. The major experiments employed in the project were the SVEKALAPKO deep seismic tomography experiment (Bock *et al.* 2001) and the BEAR electromagnetic array research (Korja *et al.* 2000).

In addition, the SVEKALAPKO project has been closely connected with the potential field studies carried out by the Geological Survey of Finland within the Crustal Model Program of Finland, aiming to answer questions concerning the geometrical, mineralogical and geological nature of the sources of potential field anomalies in the Finnish lithosphere (Korhonen *et al.* 1997). The main target of the project *Three-dimensional (3-D) crustal model of the SVEKALAPKO research area* (3-DCM project) carried out by the Geological Survey of Finland in collaboration with the Department of Geophysics of Oulu University is the joint interpretation of potential fields and SVEKALAPKO seismic data. The investigation aims to produce an integrated geophysical model of the crust of southern and central Finland (referred hereafter as the SVEKALAPKO area) that includes the distribution of *P*- and *S*-wave velocity, density and magnetization.

Previous 3-D regional density models described regional trends in the observed gravity field of Fennoscandia (Glaznev *et al.* 1996; Wang 1998). As a result of their large scale, these models represent only the major features of the distribution of density within the crust. A more detailed model is necessary to better understand the nature of local- and regional-scale gravity anomalies in Finland. In this paper, we present the 3-D crustal density model compiled for the smaller area of the SVEKALAPKO seismic array. The model was constructed by inversion of the observed Bouguer anomaly using an existing 3-D crustal *P*-wave velocity model of the SVEKALAPKO area and petrophysical data about bedrock density in Finland as *a priori* information. Previously, 2-D density models were obtained for various parts of Finland by Elo & Korja (1993), Elo (1997), Kozlovskaya & Yliniemi (1999) and Korja *et al.* (2001). A detailed 3-D density model has not been compiled for this area before.

2 THE RELATIONSHIP BETWEEN DENSITY AND SEISMIC VELOCITY AS A PRINCIPAL CONDITION OF JOINT INTERPRETATION OF SEISMIC AND GRAVITY DATA

Use of information about seismic velocities in gravity modelling requires knowledge of the relationship between rock density and seismic velocity, such as established by Birch (1961) and Nafe & Drake (1957) from measurements of rock density and seismic velocity under laboratory conditions. They demonstrated that the compressional wave velocity in an isotropic medium depends primarily on the mean atomic mass and material density. In real rocks, both seismic velocity and density are also affected by other factors, such as pressure and temperature, the rock macrostructure and microstructure, cracks and fractures, the presence of fluids and anisotropy of the rock-forming minerals. Generally, these factors affect density and velocity in different ways and this must be taken into consideration when applying density–velocity relationships established under laboratory conditions to studies of the deep structure of the lithosphere.

One of the problems in applying density–velocity relationships established under laboratory condition to integration of seismic and gravity data is significant scatter around the mean value revealed for all types of lithospheric rocks. As a result of the scatter, any density–velocity relation has to be regarded as statistically determined rather than functional.

Studies of density–velocity relation in the KTB (The German Continental Deep Drilling Program) superdeep hole (Kneib 1995; Jones & Holliger 1997) have demonstrated that the statistical properties of the density–velocity relationship depend strongly on the observation scale. At short wavelengths (less than 10 m) the correlation between velocity and density logs is very poor as result of large scatter, but the correlation improves (that is, the scatter decreases) with increasing wavelength. Consequently, we may expect that the scatter in the density–velocity relationship for geological units with a characteristic scale of more than 10 km is less than that observed in laboratory measurements on rock samples. This scaling effect should be taken into consideration in regional-scale gravity studies.

The main factor affecting seismic velocities in the upper continental crust is the presence of cracks and fractures; these are often also filled with fluids. In the Fennoscandian Shield, the upper crust is permeated by fluid-filled fractures and cracks down to a depth of at least 12 km, as demonstrated by a detailed study of rock properties in the Kola superdeep borehole (Ganchin *et al.* 1998; Smithson *et al.* 2000). As a result, seismic velocities in the upper crust are lower than intrinsic (crack-free) velocities by approximately 0.2 km s^{-1} (Smithson *et al.* 2000) and the density estimate obtained from these velocities will be biassed low by approximately 0.1×10^3 kg m^{-3}, if any standard linear density–velocity relationship is used.

In the middle and lower crust, where all the cracks are closed, the seismic velocities and densities depend on pressure and temperature, but the influence of these factors is weak compared to the influence of rock composition. In shield areas, the combined effect of pressure and temperature on seismic velocities and densities cancels out at a depth corresponding to the middle and lower crust (that is, at pressures greater than 2 kbar) (Kern & Richter 1981; Schön 1998). Therefore, both velocities and densities in the middle and lower crust depend mainly on the elastic properties of rock-forming minerals and are controlled by pressure-dependent mineral reactions changing the mineral assemblages from plagioclase-bearing and garnet-free to garnet-bearing and plagioclase-free (Green & Ringwood 1967). This results in an increase of both density and velocity with depth and a strong density–velocity correlation (Sobolev & Babeyko 1994).

3 PREVIOUS INVESTIGATIONS OF DENSITY–VELOCITY RELATIONSHIPS IN LARGE-SCALE GEOLOGICAL UNITS

Detailed analyses of the density–velocity relationship in large-scale geological structures have been compiled by Krasovsky (1981) and

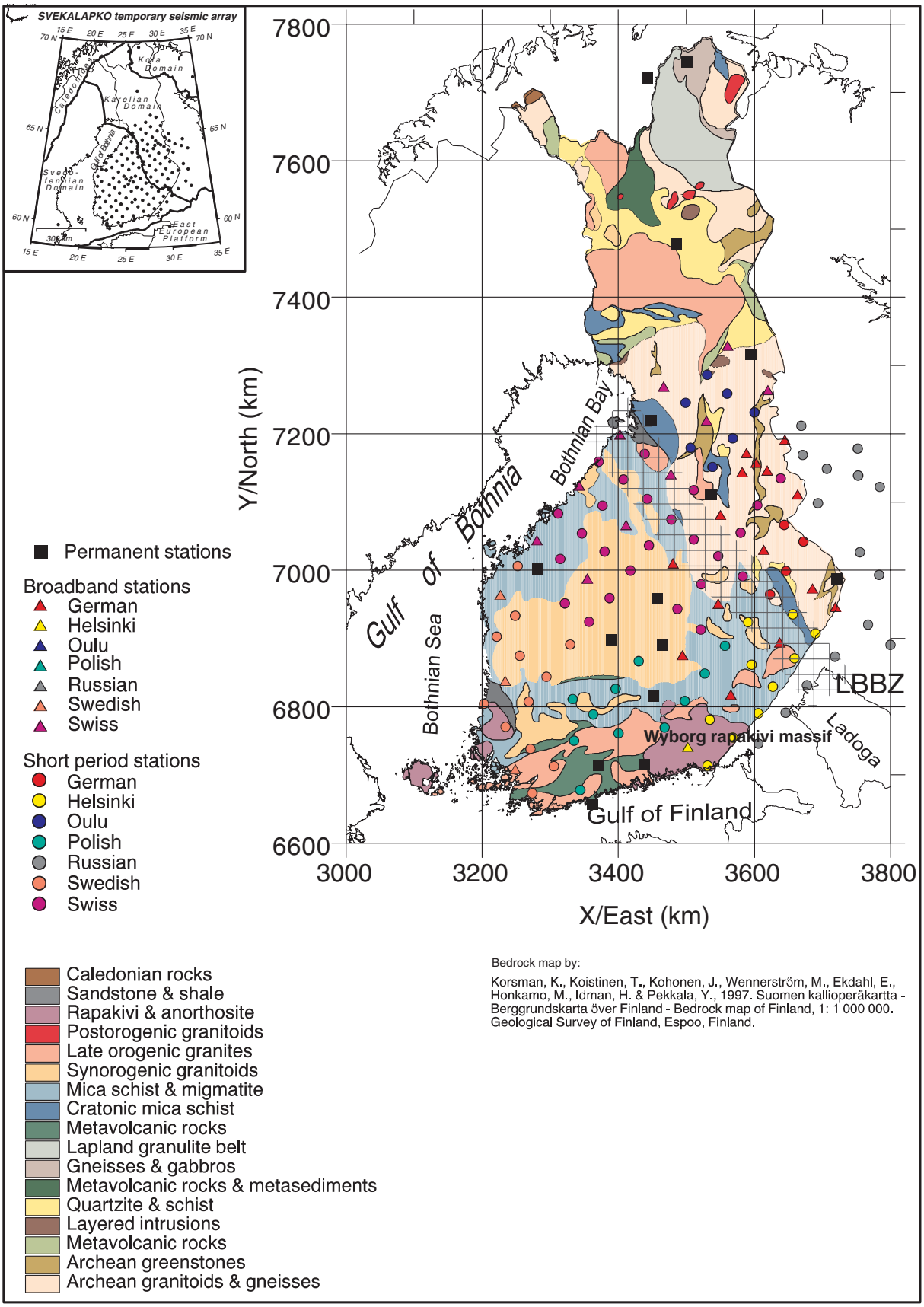

Figure 1. Location of the SVEKALAPKO temporary seismic array on the bedrock map of Finland. The map is displayed using the National Finnish Coordinate System (KKJ) (Hirvonen 1949; Ollikainen *et al.* 2001). The location of the Ladoga–Bothnian Bay zone (LBBZ) is indicated by the hatched band. The geographical position of the study area is shown in the inset, upper left corner, where the main crustal segments are separated by thick lines.

Christensen & Mooney (1995) based on the results of laboratory measurements of elastic properties.

Alternatively, the density–velocity relationship in lithospheric units of regional scale can be obtained directly from the velocity distribution within the lithosphere provided by large-scale seismic experiments and observed gravity data (Kozlovskaya & Yliniemi 1999; Kozlovskaya *et al.* 2001a,b, 2002). This approach makes it possible to find a density–velocity relationship that gives the best fit of the density model to the observed gravity data; in other words, the relationship is obtained as a solution to the inverse gravity problem.

This method has allowed investigation of the density–velocity relationship for large-scale geological units with available wide-angle reflection and refraction profiles: the SVEKA profile in Finland (Kozlovskaya & Yliniemi 1999) and the EUROBRIDGE'95-EUROBRIDGE'97 profiles (Kozlovskaya *et al.* 2001a,b, 2002), crossing a number of tectonic units of varying ages in Finland, Lithuania, Belarus and the Ukraine. The scale of lateral velocity inhomogeneities revealed by these profiles is approximately 30–100 km. The density–velocity relationship obtained for these profiles is quasi-linear in many cases, although variations in the relationship for different tectonic units resulted in scatter of *P*-wave velocity (0.2–0.5 km s^{-1}) around the corresponding values of density.

The investigations also revealed that the quasi-linearity of density-V_p relationship can be violated in some cases. For example, the density–velocity relationship may be violated as a result of seismic anisotropy in tectonically deformed rocks, as was demonstrated by the EUROBRIDGE'96 profile (Kozlovskaya *et al.* 2002).

Another case is the presence of large rapakivi–gabbro–anorthosite massifs containing abundant amounts of rocks with high feldspar content, that is rapakivi granites and anorthosites. Wide-angle reflection and refraction profiles across large rapakivi–gabbro–anorthosite massifs sometimes reveal very high values of *P*-wave velocity (up to 6.4 km s^{-1}) at upper and middle crustal depths. For example, high *P*-wave velocities in the upper and middle crust were revealed by the BALTIC profile within the Wyborg rapakivi batholith (Luosto *et al.* 1990) and by the EUROBRIDGE'97 profile within the Korosten rapakivi–gabbro–anorthosite pluton in the Ukrainian Shield (Thybo *et al.* 2003). In both cases, the areas of high *P*-wave velocity in the uppermost crust are also marked by a negative gravity anomaly. However, use of a quasi-linear V_p-density relationship results in positive values of calculated gravity above these areas.

The high *P*-wave velocity in the uppermost crust within rapakivi–gabbro–anorthosite massifs can be attributed to anorthosites. As a result of high amounts of plagioclase in these rocks, they have *P*-wave velocities comparable with those of gabbro, while their densities are significantly less (Henkel *et al.* 1990; Kern *et al.* 1993). The high *P*-wave velocity may also be the result of the influence of pressure on the *P*-wave velocity of rapakivi granites. Extensive laboratory studies of elastic properties of granitoids of the Ukrainian Shield under confining pressures and temperatures corresponding to the present-day geotherm Lebedev *et al.* 1972; Lebedev *et al.* 1983; Lebedev 1985; Lebedev *et al.* 1986; Schön 1998) demonstrated strong dependence of *P*-wave velocity on rock texture. The highest pressure effect was found in coarse-grained rapakivi granites, in which V_p increases rapidly from approximately 6.0 km s^{-1} at a depth of 0 km up to 6.5 km s^{-1} at a depth of approximately 5 km. In fine- and medium-grained granites the effect of pressure on V_p is much less.

As a result of this anomalous behaviour of *P*-wave velocity in rapakivi granites, they cannot be distinguished from more dense anorthosites if V_p values only are used. However, the *S*-wave velocity (V_s) in rapakivi granites is generally less affected by the pressure and temperature in the same depth interval (Lebedev *et al.* 1986). That is why use of both V_p and V_s makes it possible to distinguish rapakivi granites from anorthosites and to obtain more realistic density models for large rapakivi–gabbro–anorthosite massifs (Kozlovskaya *et al.* 2001b).

4 GRAVITY DATA

For the present study, maps of Bouguer gravity anomaly and its regional residual (Figs 2a and b) were compiled on a 100 km^2 regular grid from the national gravity net of the Finnish Geodetic Institute (Elo 1997; Kääriäinen & Mäkinen 1997; Korhonen *et al.* 2002). The regional residual was obtained by continuation of the Bouguer anomaly map upward to an altitude of 10 km, using Geosoft Oasis 5.0 software. The average linear spacing of observational stations is 5 km. The gravity values were tied to the International Gravity Standardization Net 1971 (IGSN71) and normalized with respect to the International Gravity Formula 1930 minus 14.0 mgal (1 mgal $= 10^{-5}$ m s^{-2}) (Elo 1997; Kääriäinen & Mäkinen 1997; Korhonen *et al.* 2002). The average value of the Bouguer anomaly in the region is -27.94 mgal. As the topography in the region is very flat, its effect is not considered in our study.

An analysis of the Bouguer anomaly map of Finland and its correlation with surface density was given by Elo *et al.* (1978) and Elo (1997). It was demonstrated that many of the large-scale gravity anomalies (several tens of kilometers) are associated with shallow structures, which correlate well with surface geology (mafic intrusions, greenstones, schist belts, anorogenic granitic intrusions, impact structures etc.). Similarly, the recent results of reflection and refraction profiles in Finland (SVEKA, BALTIC, FENNIA) and in the western part of the East European craton (EUROBRIDGE'95–97) showed that lateral velocity variations in the upper crust with characteristic lateral sizes of approximately 30–100 km demonstrate good correlations with Bouguer anomalies of the same scale in many cases, although the amplitude of these anomalies cannot always be explained by shallow structures only (Elo 1997; Kozlovskaya & Yliniemi 1999; Kozlovskaya *et al.* 2001a,b, 2002). This observation forms the background for the use of *P*-wave velocity data to calculate the density model of the SVEKALAPKO array area.

5 THE EXISTING *P*-WAVE CRUSTAL VELOCITY MODEL OF THE SVEKALAPKO ARRAY AREA AND THE MAJOR BOUNDARIES IN THE CRUST

The *a priori* 3-D *P*-wave velocity model of the crust for the area of the SVEKALAPKO seismic array was compiled by Sandoval (2002), based on the results of previous controlled-source seismic (CSS) experiments in the Fennoscandian Shield (Fig. 3). The model was created mainly for the purpose of estimating the effect of the crust on teleseismic wavefront propagation, but it can be also used for gravity data modelling.

The 3-D model (Fig. 4) was obtained using B-spline interpolation of the velocity values and main seismic interfaces between profiles. See Sandoval (2002) and Sandoval *et al.* (2003) for details. The two main velocity boundaries in the model are the Moho and the high-velocity lower crust with $V_p > 7.0$ km s^{-1}, which is spread beneath the Proterozoic Svecofennian part of the area studied, but is practically absent from the Archaean domain (Korja *et al.* 1993). The values of velocity in the model were calculated on an 8-km^3

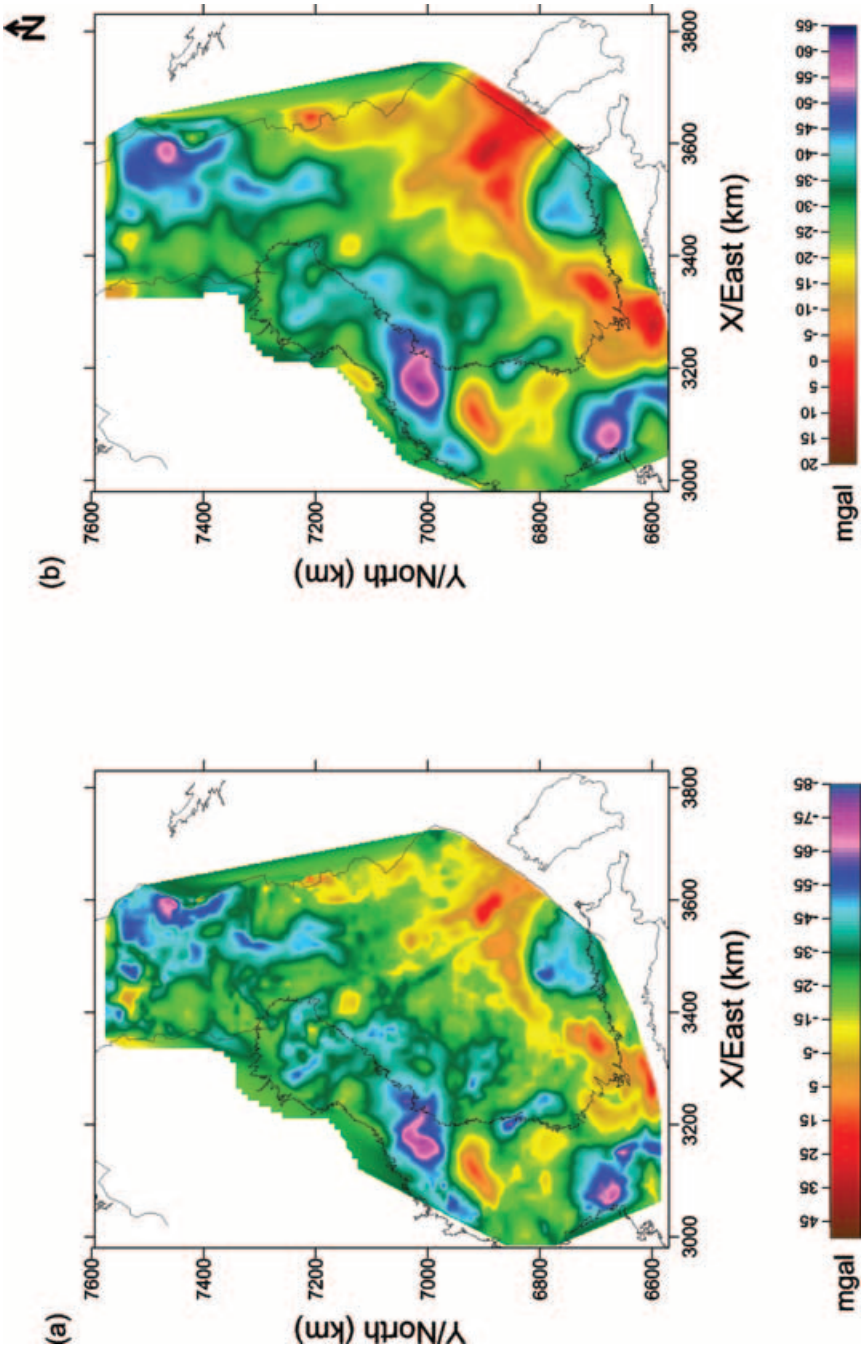

Figure 2. Gravity field in the area under study: (a) Bouguer anomaly map, (b) Bouguer anomaly continued upward to 10 km. The digital maps have been compiled by J. Korhonen from the data of the Finnish Geodetic Institute and are displayed using the National Finnish Coordinate System (KKJ). The values of the gravity field are in units of mgal (10^{-5} m s^{-2}).

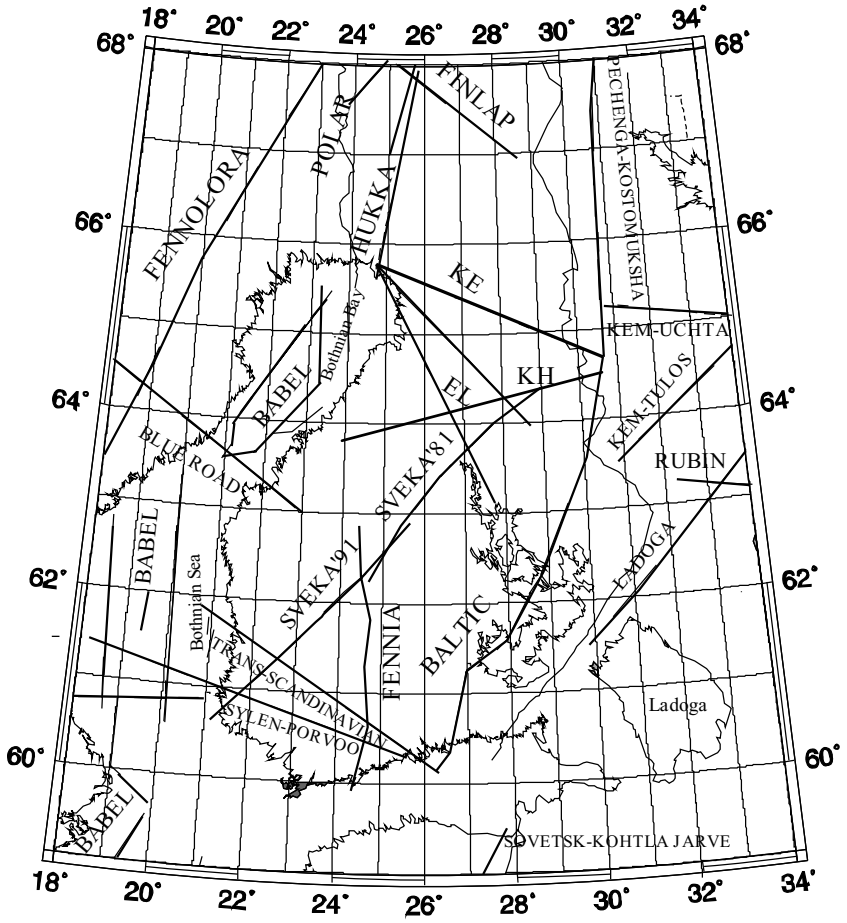

Figure 3. Location of previous controlled-source seismic (CSS) profiles used to produce the initial crustal *P*-wave velocity model (after Sandoval 2002).

(that is, 2 × 2 × 2 km) regular grid to represent adequately the variations of depth to the velocity interfaces.

Within this model, the Moho has two large depressions beneath central and southern Finland and the Gulf of Bothnia. That is in agreement to the previous result by Luosto (1991) and more recent data about the Moho depth in the region obtained independently by Alinaghi *et al.* (2003) from teleseismic receiver function analysis of the SVEKALAPKO array data. The third narrow Moho depression in the northern part of the SVEKALAPKO area is more clearly expressed in the model of Sandoval (2002) than in the earlier map of Luosto (1991), because additional results of seismic profiling in northern Finland (Yliniemi 1991) were used for compilation of the new model.

As only two velocity interfaces were included in Sandoval's model, its upper part does not contain the information about vertical and lateral velocity variations in the upper and middle crust in the various tectonic units documented by previous near-vertical and wide-angle reflection and refraction seismic experiments in the area (Luosto *et al.* 1984, 1990; Yliniemi 1991; BABEL Working Group 1993, Yliniemi *et al.* 1996; Luosto 1997; Kozlovskaya & Yliniemi 1999; Berzin *et al.* 2002). This may affect the results of gravity modelling because gravity data is particularly sensitive to shallow structures.

A comprehensive analysis of recordings of previous wide-angle reflection and refraction profiles in Finland was made by Luosto (1997) and Pavlenkova *et al.* (2001). They identified three main branches of the first arrivals with apparent velocities of 6.0–6.4, 6.5–6.6 and 6.8–7.0 km s^{-1} that define three main crustal layers (upper, middle and lower crust) on all profiles. In the areas of deep Moho (greater than 50 km) an additional high-velocity lower crustal layer with velocities in excess of 7.0 km s^{-1} appears (Luosto 1997). Based on this observation, the crust in Finland can be generally subdivided into four layers named upper crust, middle crust, lower crust and high-velocity lower crust, with V_p of 6.0–6.4, 6.4–6.8, 6.8–7.0 and 7.0–7.7 km s^{-1}, respectively. This general subdivision of the crust into four layers, instead of two or three, is in agreement with other results of seismic wide-angle reflection and refraction profiling in Precambrian areas (see, for example, Hall *et al.* 2002; Kozlovskaya *et al.* 2002), demonstrating similar features of the velocity distribution within the crust.

In addition to strong reflections from the Moho, the upper/middle crust boundary is clearly seen in many record sections of wide-angle reflection/refraction profiles in Finland. Specifically, at offsets of 80–120 km the first arrivals are strongly attenuated and a high-amplitude secondary wave appears with a delay of 0.2–0.4 s. For some profiles this wave pattern was explained by a low-velocity layer with a thickness of several kilometers separating the upper crust from the middle crust (Luosto *et al.* 1984; Berzin *et al.* 2002). The depth to the upper boundary of the layer varies from 5 to 15 km in different profiles. It is not clear, however, whether the low velocity of the layer can be explained by a variation in rock composition, as the velocity and thickness of the layer are poorly constrained by refraction data. Berzin *et al.* (2002) proposed that it might alternatively be explained by a layer with increased porosity. Therefore,

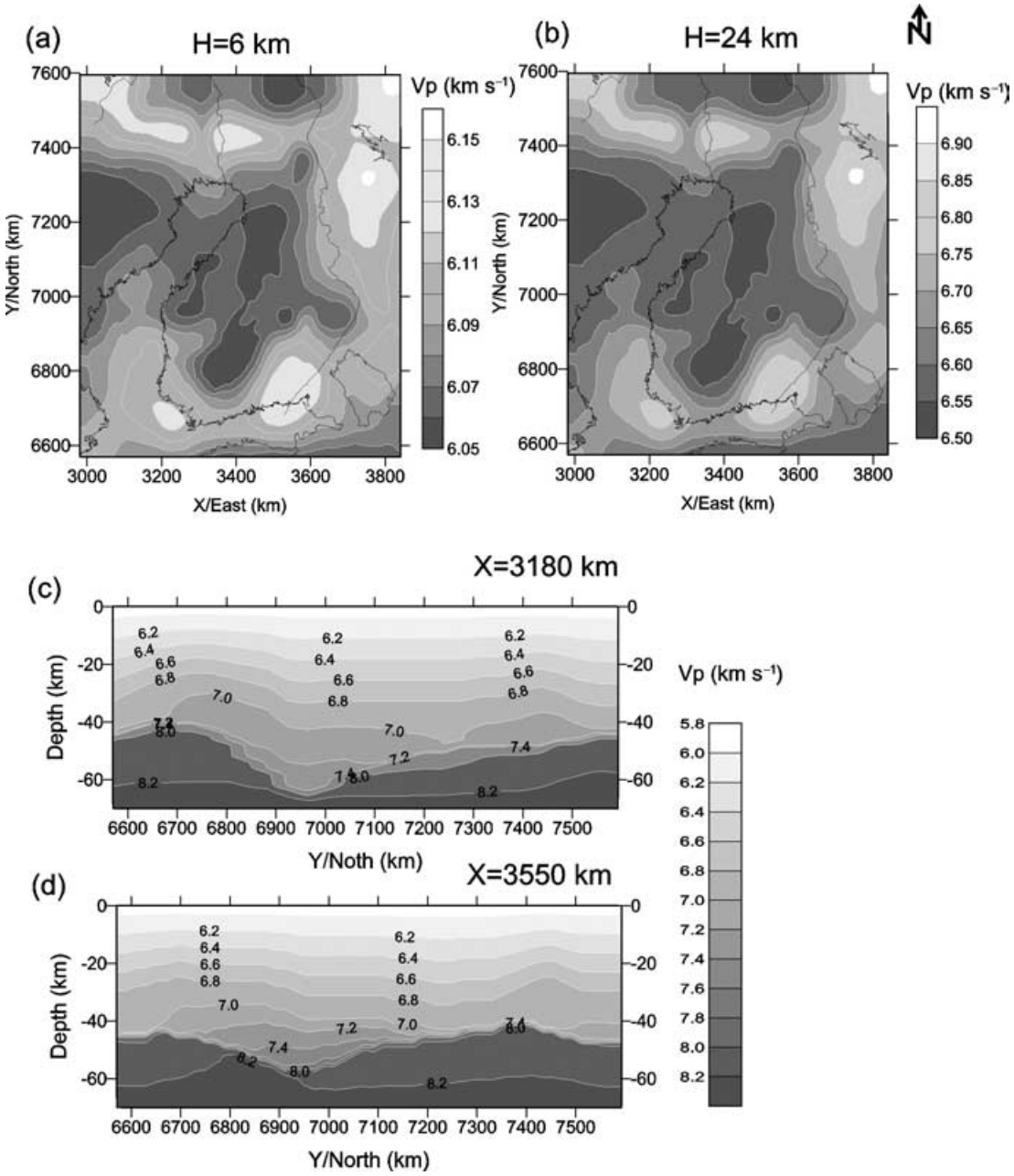

Figure 4. Horizontal (a, b) and vertical (c, d) cross-sections through the crustal 3-D *P*-wave velocity model of Sandoval (2002) defined on 8 km^3 rectangular grid. The coordinates of the grid were calculated using transformation of geographical WGS-84 coordinated into the National Finnish Coordinate System (KKJ).

the upper/middle crust boundary may be associated with the lower boundary of this layer located at a depth of 10–20 km in the study area.

The middle/lower crust boundary and lower/high-velocity-lower crust boundary are not so clear as the Moho and the upper/middle crust boundary. In record sections of wide-angle reflection/refraction profiles, they are usually seen as strong amplitude secondary arrivals that can be correlated over distances of 30–100 km. These boundaries were interpreted as subhorizontal or gently inclined.

It is important to note that the main intracrustal boundaries revealed by wide-angle reflection/refraction profiling in the region are not seen as continuous subhorizontal reflectors in record sections of near-vertical reflection profiles. However, in many cases they can be distinguished as a change in reflectivity pattern that occurs at approximately the same depth as the main subhorizontal boundaries in wide-angle reflection/refraction velocity models (BABEL Working Group 1993; Berzin *et al.* 2002). This indicates that these boundaries are not sharp velocity discontinuities caused by lithological contact, but rather transition zones or zones of high-velocity gradient several kilometers in thickness. Such transition zones can be the result of a gradual change in rock composition or in metamorphic grade that results also in a gradual increase of seismic velocity and density with depth.

As it was demonstrated by Christensen & Mooney (1995), the gradual increase of seismic velocities and density with depth in

stable continental crust can be explained in terms of both change in rock composition from felsic to mafic mineral assemblages and increase of the metamorphic grade. Therefore, the upper crust in Finland with V_p of less than 6.4 km s^{-1} can be considered as composed mainly of rocks of felsic composition and low metamorphic grade. The middle crust with V_p of 6.4–6.8 km s^{-1} is composed of rocks of intermediate composition, in which the metamorphic grade increases with depth from amphibolite to granulite facies. The lower crust with V_p of 6.8–7.0 km s^{-1} contains abundant amounts of dense, mafic, granulite-facies rocks, in which garnet content increases with depth, while the high-velocity lower crust with V_p of 7.0–7.7 km s^{-1} is most probably composed of denser, mafic, garnet granulites and eclogites.

It should be noted, however, that the term lower crust has been applied to various seismic layers in previous papers devoted to the structure of the crust in Fennoscandia. This has resulted in controversy regarding the thickness and depth of the mafic lower crust. For example, in the monography by Wang (1998), the mafic lower crust is a combination of the high-velocity lower crust with the layer with *P*-wave velocities of 6.8–7.0 km s^{-1}. Korja *et al.* (1993) and Korsman *et al.* (1999) defined the lower crust as the layer with $V_p >$ 7.0 km s^{-1}. However, they also defined the lower crust as the layer with $V_p > 6.8$ km s^{-1} in the areas from which the high-velocity lower crust is absent or is very thin. Glaznev *et al.* (1996) considered the mafic lower crust as a layer with V_p of 6.4–7.0 km s^{-1}, while the layer with $V_p > 7.0$ km s^{-1} was considered as an additional, transitional crust–mantle layer. Henkel *et al.* (1990) assumed that the mafic lower crust is a layer with an average value of V_p of 6.8 km s^{-1} and the layer with $V_p > 7.0$ km s^{-1} was modelled as a number of additional eclogitic bodies at the base of the crust. Sandoval (2002) used the definition of the lower crust proposed by Korja *et al.* (1993) and Korsman *et al.* (1999) for the *P*-wave velocity model of the crust of the SVEKALAPKO area.

As there are varying points of view on the depth to the mafic lower crust in the area and its thickness, in our study we considered two different *P*-wave velocity models, in which two different definitions of the lower crust were used. The first was the model of Sandoval (2002), in which the lower crust is a layer with $V_p > 7.0$ km s^{-1}. In the second, we considered the mafic lower crust as consisting of two layers with V_p of 6.8–7.0 and 7.0–7.7 km s^{-1}, respectively.

6 THE GRAVITY EFFECT OF THE INITIAL 3-D CRUSTAL *P*-WAVE VELOCITY MODEL

Variations of density in the upper crust have a significant effect on the observed Bouguer anomaly, which is why uppermost crustal density inhomogeneities should be taken into consideration in the regional gravity studies. However, in many cases the values of V_p in the upper crust are underestimated from wide-angle reflection and refraction profiles. One reason for this is the influence of fracturing on seismic velocities, as discussed in Section 3. In addition, all wide-angle reflection/refraction profiles in Finland had excessive distances between shot points (approximately 70 km), which resulted in poor velocity resolution for the upper crust. So additional information about mass sources in the upper crust should be used to improve the fit of the calculated gravity field to the observed Bouguer anomaly.

To assign the density values in the upper crust, we used the map of bulk density of bedrock of Finland (Fig. 5a) compiled by Korhonen *et al.* (1997). The statistical properties of the density of bedrock in Finland were estimated by Elo (1997). He pointed out that the histogram of the density distribution is trimodal, with the main component corresponding to granodiorites with a mean density of 2.69×10^3 kg m^{-3}, a low-density component corresponding to granites and granite gneisses with the mean density of 2.612×10^3 kg m^{-3}, and a high-density component corresponding to high-grade metamorphic, mafic intrusive and volcanic rocks with a mean density of 2.795×10^3 kg m^{-3}. The average surface density of the bedrock in Finland is 2.71×10^3 kg m.

Because of the lack of detailed information about the geometry of 3-D upper crustal sources, which is known only along 2-D seismic profiles in the region, the variations of density in the upper crust in our model were represented by vertical bodies, having density values equal to those from the density map and continued downwards to the upper/middle crust boundary. Our selection of such an approximation for the upper crust is based on a recent analysis of crustal reflectivity from different tectonic units worldwide made by Meissner & Rabbel (1999). They pointed out that the crystalline upper crust of cratonic terrains generally exhibits only one of two types of reflectivity. It is either transparent or/and it shows traces of thrusts and shear zones of former or present ruptures that are usually seen as rather steeply inclined structures. The transparency, in turn, may be caused either by low impedance contrast within the mainly felsic rocks or by steep inclination of folded or faulted layers (apparent transparency). Record sections of the reflection seismic surveys in the study area (BABEL Working Group 1993; Berzin *et al.* 2002) demonstrate the same main types of reflectivity in the upper crust.

These types of reflectivity indicate that vertical and subvertical structures generally prevail in the upper crust. Reflectivity corresponding to horizontal lamination may occur on local scales as a result of the presence of mafic sills. However, regional-scale horizontal layering is usually observed within sedimentary basins and has never been detected in crystalline upper crust.

Approximation of upper crustal sources by equivalent mass distribution is a better alternative to the low-pass filtering of the short-period component from the data. As can be seen from Fig. 2(a), many of the large-scale anomalies in the area are marked also by a high horizontal gradient, indicating that the upper boundary of the corresponding masses is located near the surface. Low-pass filtering would smooth the areas with high horizontal gradient, projecting the shallow sources to a greater depth.

The values from the map shown in Fig. 5(a) were used to correct the density values in the upper crust. Then the gravity effect of the crust was calculated using the technique of Kozlovskaya *et al.* (2001a). As it was discussed in Section 5, the upper/middle crust boundary is located at an average depth of approximately 15 km in our study area. As the model of Sandoval (2002) does not include this boundary, we assumed that the lower boundary of the masses in the upper crust coincides with the 6.2 km s^{-1} velocity isoline located at a depth of approximately 8–12 km, that is, approximately at the same depth as the seismically detected upper/middle crust boundary (Fig. 5b).

Fig. 5(c) demonstrates the gravity effect of the upper crust calculated under the assumption that the density below the upper/middle crust boundary is constant and equal to the average density of the bedrock in Finland (2.71×10^3 kg m^{-3}). Fig. 5(d) shows the total gravity effect of the whole 3-D crustal model corrected for the upper crustal sources. The gravity effect was calculated using the technique of Kozlovskaya *et al.* (2001a). A large negative anomaly can be seen in the central part of the study area. The location of this anomaly indicates that its source is a mass deficiency in the area of the deepest Moho. That is, the high-velocity lower crust together

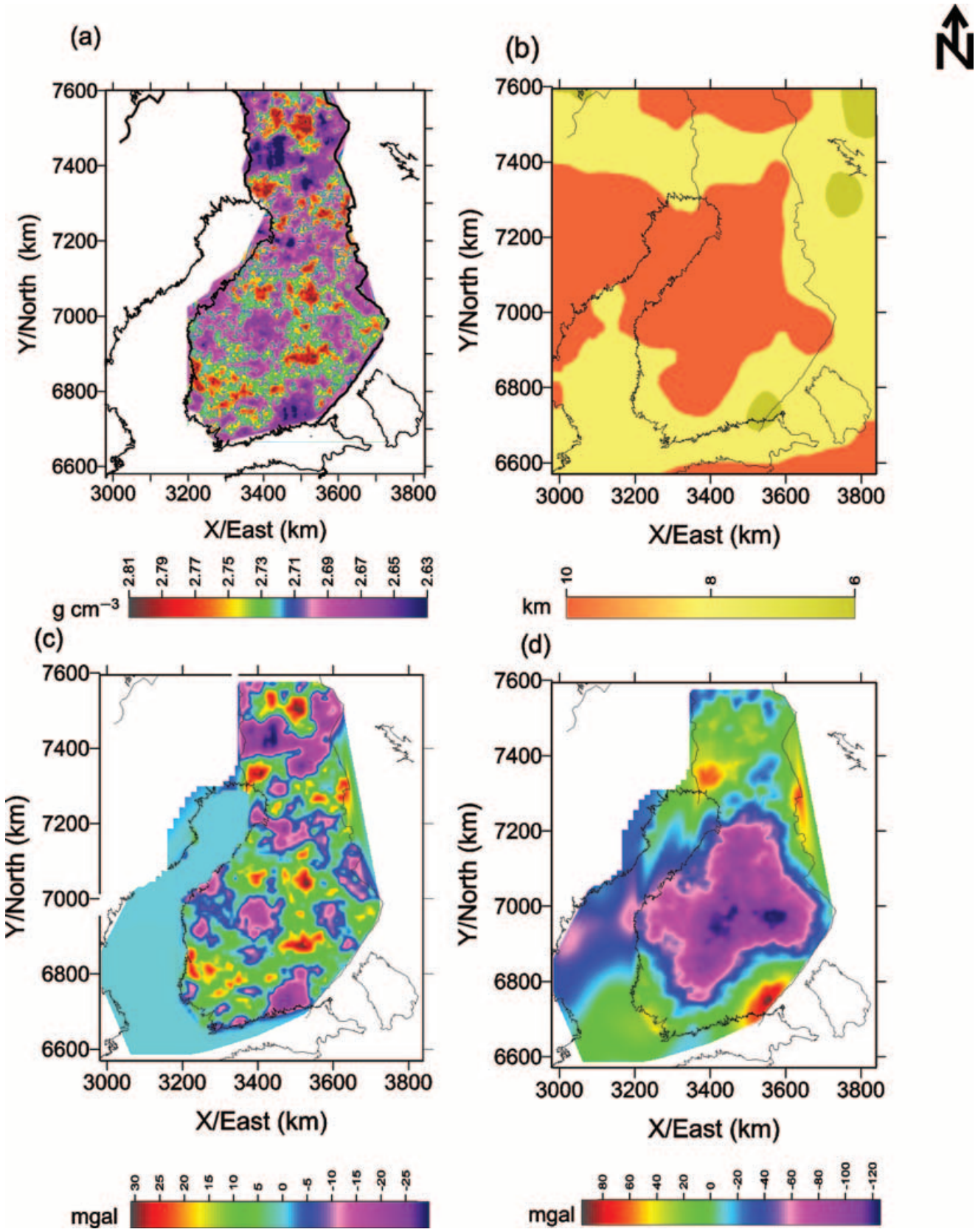

Figure 5. Input data and results of gravity modelling using the crustal *P*-wave velocity model of Sandoval *et al.* (2003): (a) map of bulk density of bedrock of Finland (after Korhonen *et al.* 1997); (b) depth to the 6.2 km s^{-1} velocity isoline (in km), assumed to be the lower boundary of uppermost crustal layer (that is, the upper/middle crust boundary); (c) the gravity effect of the uppermost crustal layer calculated under the assumption that the density beneath the upper/middle crust boundary is constant; (d) the calculated gravity effect of the whole crustal model. The density values are given in 10^3 kg m^{-3}. The values of the gravity field are in units of mgal (10^{-5} m s^{-2}).

with the sources in the upper crust do not completely compensate the Moho depression. The edges of the anomaly are rather sharp, indicating that its source is located somewhere in the upper or middle crust. This is in agreement with the previous analysis made by Elo (1997), who showed that a considerable mass surplus must exist in the upper and middle crust to compensate the deepest Moho. Thus, more detailed information about velocity values in the upper and middle crust should be added to the initial velocity model in order to improve agreement with the observed gravity data.

To investigate the effect of uncertainty in the location of the upper/middle crust boundary on the calculated gravity effect of the crust, we performed a series of calculations assuming that the lower boundary of the masses in the upper crust was located at different depth, that is coinciding with the 6.2, 6.3 and 6.4 km s^{-1} velocity isolines, respectively. They demonstrated that variations in the depth of the upper/middle crust boundary have only a minor effect on the anomaly in the area of the deepest Moho.

To compare the calculated effect of the upper crust to the observed Bouger anomaly, we estimated the correlation of the calculated gravity effect resulting from the upper crust with the local component of the Bouguer anomaly obtained as the residual of the observed Bouguer anomaly after substraction of its regional component shown in Fig. 2. The correlation coefficient of these two data sets is 0.1427. The weak spatial correlation of the calculated gravity effect with the local component of the Bouguer anomaly is mainly the result of the interpolation used to produce the bulk density map: as the sampling grid was irregular, the interpolation of the density values onto a regular 4-km^2 grid resulted in enhancement of some high- and low-density anomalies. Another reason for the disagreement may be that some of the local anomalies are caused by shallow sources that are not exposed.

7 MODIFICATION OF THE CRUSTAL VELOCITY MODEL

As discussed in Section 5, the crust in Finland can be considered as consisting of four major layers separated by transition zones. In accordance with the results by Korja *et al.* (1993), Luosto (1997), Korsman *et al.* (1999) and Pavlenkova *et al.* (2001), the depth to the high-velocity lower crust generally varies from 34 to 38 km and has an antiform strucrure with respect to the Moho depth. The depth to the middle/lower crust boundary generally follows the same trend and is 27–30 km. The depth to the upper/middle crust boundary varies over a wide range of 10–20 km. For example, in the velocity models along the extended SVEKA profile (Yliniemi *et al.* 1996; Kozlovskaya & Yliniemi 1999) and the EL (Elijärvi-Lahnaslampi) profile (Yliniemi 1991) the depths to the upper/middle crust boundary and middle/lower crust boundary are 11 km and 24 km, respectively. The depths to these boundaries decreases above the Moho depression, where high values of bedrock density at the surface are also observed (Elo 1997; Kozlovskaya & Yliniemi 1999).

The decrease in depth of the 6.4 and 6.8 km s^{-1} velocity isolines above the southern part of the Moho depression in the Gulf of Bothnia also was revealed by wide-angle data on the BABEL1 profile (Graham *et al.* 1992; Heikkinen & Luosto 2000). Deepening of these isolines is detected in the northern part of the Moho depression, where a dipping intracrustal reflector and a change in reflectivity pattern compared to the southern part are also observed in the near-vertical reflection record section.

Taking all the results mentioned above into consideration, we corrected the initial crustal model by introducing two additional boundaries into the crust, an upper/middle crust boundary and a middle/lower crust boundary. The boundaries were interpolated to the initial 8-km^3 grid (Fig. 6). *P*-wave velocities in the upper, middle and lower crust were taken to be 5.9–6.4, 6.4–6.8 and 6.8–7.0 km s^{-1}, respectively. The values of velocity between these boundaries were calculated using a linear 1-D vertical interpolation. Such a subdivision of the crust into four layers can be considered an approximation of the real velocity distribution. That is, large-scale lateral velocity inhomogeneities within the crust are approximated by the variations of depth to these boundaries. It also represents better the gradual increase of seismic velocity with depth.

To correct the density values in the upper crust, the absolute values of density were initially taken from the bulk density map, but the location and shape of high- and low-density anomalies were defined using the local gravity field component. The other condition used was an adjustment to the statistical properties of the density of bedrock in Finland described by Elo (1997). Additional information about large-scale positive velocity anomalies in the upper crust was also provided by interpretation of *P*-waves of local events data of the SVEKALAPKO seismic array (Yliniemi *et al.* 2004). It revealed several high-velocity anomalies in the crust, which are located along the Ladoga–Botnian Bay zone (Fig. 1) and are also spatially coincident with the corresponding positive Bouguer anomalies. A further high-velocity anomaly in the upper crust was also found in the area of the Wyborg rapakivi–anorthosite massif (Fig. 1) where the large negative Bouguer anomaly is observed (Fig. 2). This high-velocity anomaly is in agreement with an earlier result obtained for the BALTIC profile by Luosto *et al.* (1990). As discussed in Section 3, these high values of V_p may be the result of anomalous behaviour of rapakivi granites under high pressure. To avoid the positive effect of these high velocities on the calculated gravity anomaly we assumed that the 6.4 km s^{-1} velocity isoline dips beneath the Wyborg massif. In other words, no high surface density was assigned to this area.

Mesoproterozoic (Jotnian) sedimentary rocks in the area are mainly located in the area of the Gulf of Bothnia (Kohonen & Rämö 2002). Unfortunately, their precise geometry is poorly known and not sufficient for the purpose of 3-D gravity study. The only seismic evidence of relatively deep sedimentary rocks here are the migrated sections along the BABEL1 line of White (1996) and Klaeshen & Flueh (1996), demonstrating that the thickness of sediments can reach 4 km. The sediments in the Gulf of Bothnia are most probably composed of sandstones, limestones, siltstones, claystones and conglomerates having rather high densities, i.e. $2.57–2.8 \times 10^3$ kg m^{-3} (Elo *et al.* 1978). As these values are generally similar to those for the bedrock, we did not introduce a special sedimentary layer into our model. The corrected density map is shown in Fig. 7.

8 DENSITY MODEL CALCULATED FROM THE CORRECTED VELOCITY MODEL

The density model was obtained from the corrected velocity model using the gravity data inversion technique described in the paper by Kozlovskaya *et al.* (2001a). In this algorithm, the density distribution is approximated by a linear combination of functions calculated from *a priori* data. In our study, the 3-D density distribution was approximated by the following expression:

$$\sigma(x, y, z) = \sum_{i=0}^{6} a_i U_i(x, y, z), \quad (1)$$

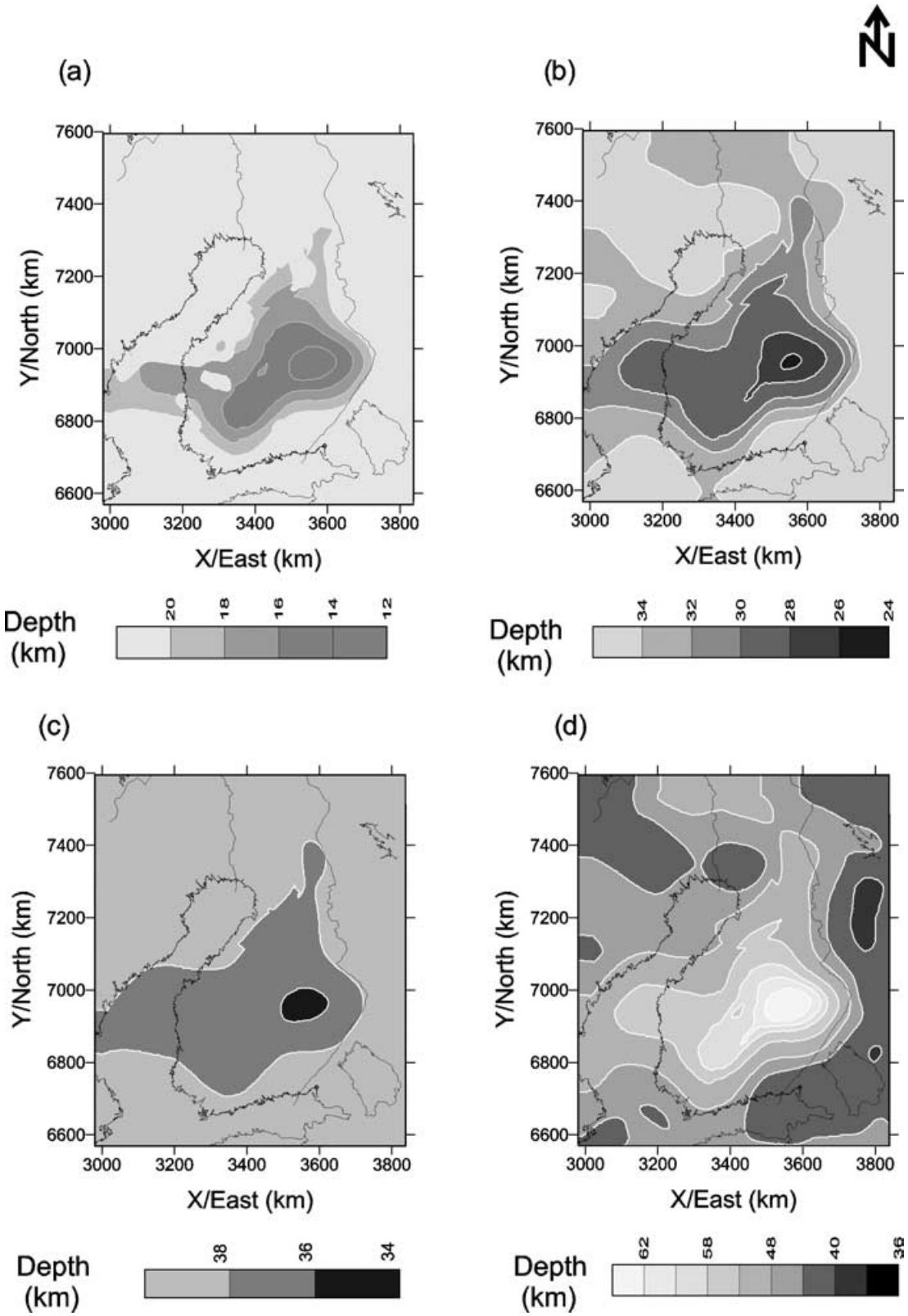

Figure 6. Corrected *P*-wave velocity model of the SVEKALAPKO area constructed as follows: (a) depth to the 6.4 km s^{-1} velocity isoline assumed as the upper/middle crust boundary; (b) depth to the 6.8 km s^{-1} velocity isoline assumed as the middle/lower crust boundary; (c) depth to the 7.0 km s^{-1} velocity isoline assumed as the lower/high-velocity-lower crust boundary; (d) depth to the Moho boundary (after Sandoval 2002); (e) and (f) vertical cross-sections of the velocity model along two selected profiles.

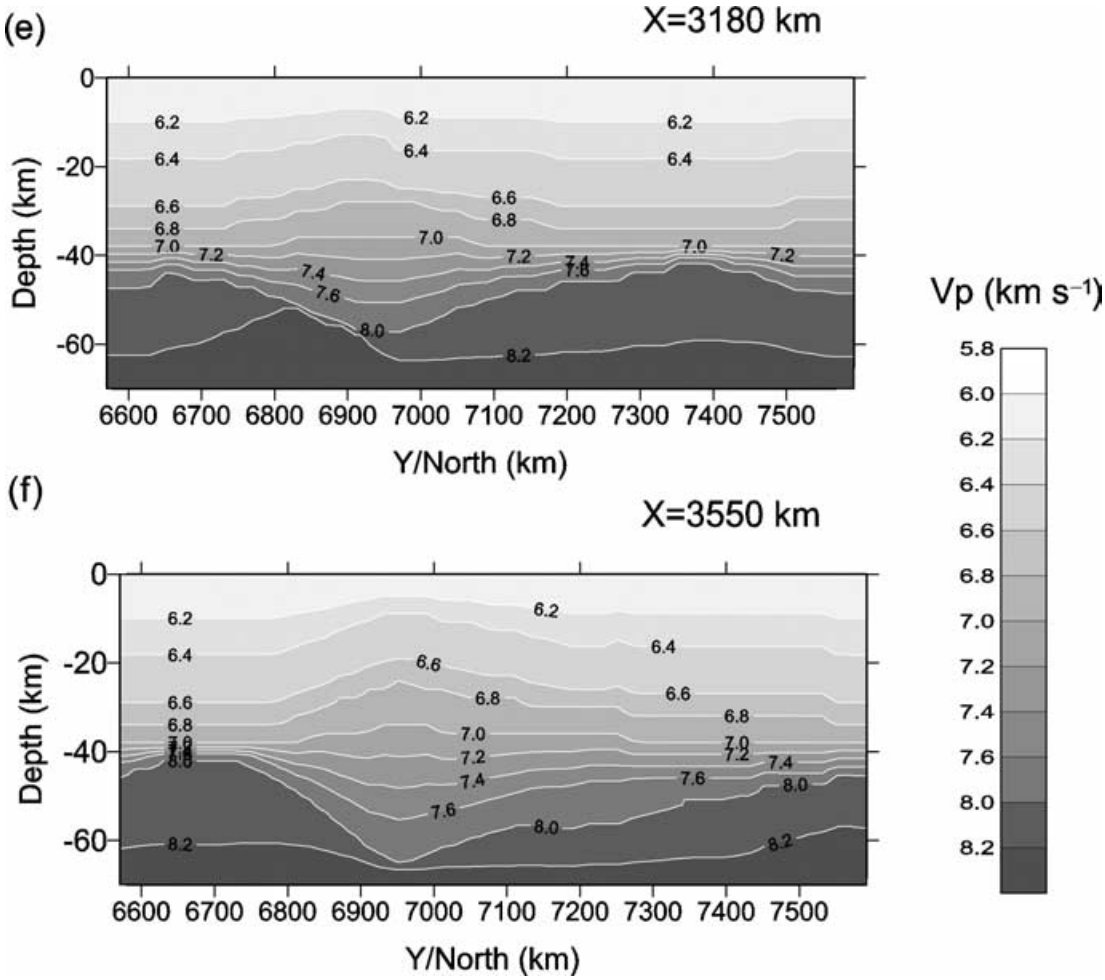

Figure 6. (*Continued.*)

where a_i are unknown coefficients, $U_0(x, y, z) = 1$, $U_1(x, y, z) = V_p(x, y, z)$ is the 3-D velocity model, $U_2(x, y, z) = H_1(x, y)$ is the depth to the upper/middle crust boundary, $U_3(x, y, z) = H_2(x, y)$ is the depth to the high-velocity lower crust, $U_4(x, y, z) = H_3(x, y)$ is the depth to the Moho boundary, $U_5(x, y, z) = V_p^{\text{aver}}(x, y)$ is the V_p averaged along the z-axis and $U_6(x, y, z) = 1/V_p(x, y, z)$.

The original 2-D computer code was modified for the case of 3-D models (see Appendix). The new version of the code also uses the non-linear optimization algorithm of Kozlovskaya (2000) instead of the solution of linear systems used in the 2-D version. The algorithm allows *a priori* information about model parameters to be introduced into the inversion algorithm and solutions corresponding to non-realistic density distributions to be rejected.

Fig. 8 shows the calculated gravity effect resulting from the crustal density distribution obtained as a result of gravity data inversion (Fig. 8a) and the residual of the observed Bouguer anomaly after removal of the calculated gravity effect resulting from the model (Fig. 8b). The RMS difference between the Bouguer anomaly and the calculated gravity is 8.63 mgal. The largest positive values of the residual are found in the northern part of the model where no reliable seismic information about Moho depth and velocity distribution within the crust is available. The negative residuals in the eastern part of the model are mainly the result of the boundary effect, that is, the lack of information about the density distribution in the upper crust outside the area covered by the gravity data. The negative residuals indicate that some of the high-density anomalies in the upper crust probably continue into Russia. The lack of information about the depth and density of sedimentary rocks in the region also affected the fit between the model field and the observed data in some places.

To demonstrate the role of different layers on compensation of Moho depression, we calculated the gravity effect of the crust, from which we removed various combinations of crustal layers (Fig. 9). Fig. 9(a) represents the calculated gravity effect resulting from a model consisting of the upper mantle and a crust with uniform density. Fig. 9(b) shows the gravity effect of a model consisting of the upper mantle, the high-velocity lower crust and a layer with uniform density above the high-velocity lower crust. Fig. 9(c) demonstrates the gravity effect of a model consisting of the upper mantle, the high-velocity lower crust, the lower crust, the middle crust and an upper crust with uniform density. The calculated gravity effects are referred to the average value of Bouguer anomaly in the region (see Appendix).

Fig. 10 demonstrates horizontal cross-sections of the model at different depths, corresponding to the upper, middle and lower crust and the upper mantle. Fig. 11 illustrates the vertical cross-sections along four profiles through the density model. The locations of the profiles were selected to demonstrate the compensation of the largest Moho depressions by high-density rocks in the crust. It should be noted that vertical stripes and spikes seen in the sections are not

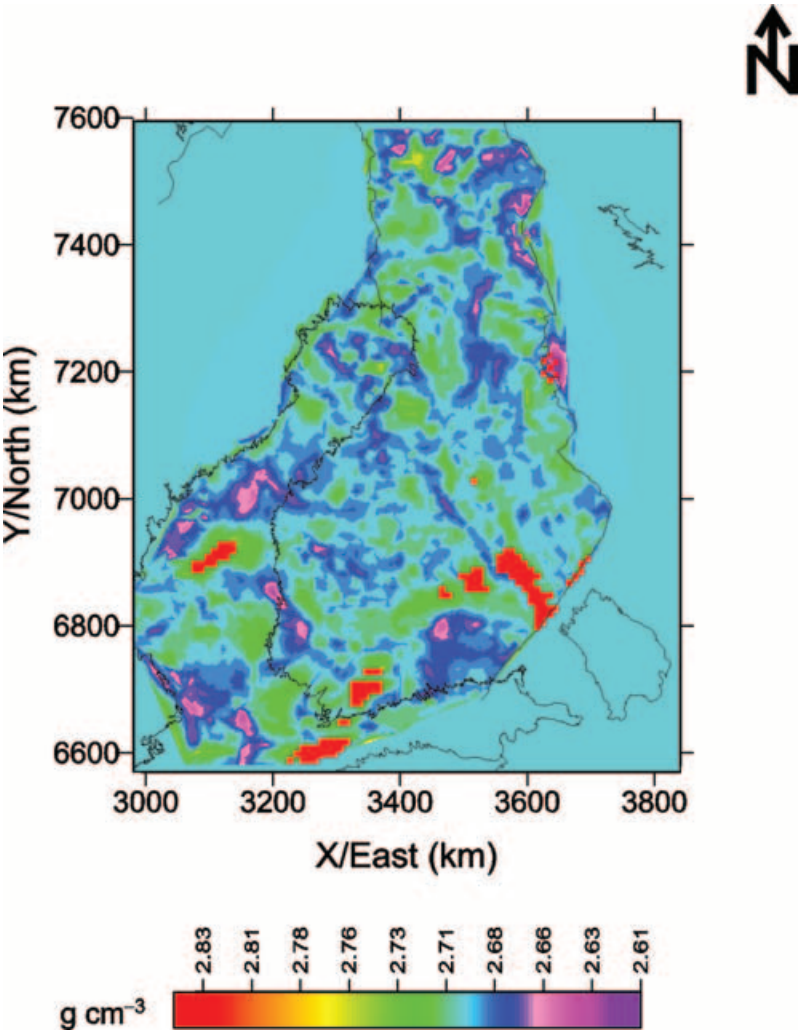

Figure 7. The density distribution at the surface derived from the local component of the Bouguer anomaly. The density values are given in units of 10^3 kg m^{-3}.

artefacts; they result from the complicated 3-D geometry of the model. Specifically, the stripes in the upper crust correspond to vertical 3-D bodies with different densities. In some places thin spikes occur as a result of the adjacent crustal blocks with significantly different structures.

9 DISCUSSION

The results of the present investigation demonstrate that a detailed Moho relief model is a very important constraint for the regional 3-D gravity modelling. Although there is no correlation between the regional Bouguer anomalies and the Moho depth in the region, the large-scale Moho depressions in the region coincide with crustal blocks with density distributions with a different character, as can be seen on Figs 10 and 11. These depressions are also associated with the presence of additional compensating masses within the crust and can be overcompensated or undercompensated, resulting in maxima or minima of the gravity field, respectively.

The second important constraint is the density contrast at the Moho boundary and the absolute values of density both in the mantle and in the lower crust. In regional gravity studies (see, for example, Gutscher 1995; Nielsen *et al.* 2000; Hofmann *et al.* 2003) the lower crust is often assumed to be composed mainly of mafic granulites and to have a density of about 2.9–3.0 $\times$ 10^3 kg m^{-3}. Recent results from seismic experiments in the Precambrian areas have demonstrated, however, that two different types of lower crust can be distinguished. In areas of relatively thin and flat Moho (40–45 km) typical values of *P*-wave velocity and density in the lower crust are close to 7.0 km s^{-1} and 3.0 $\times$ 10^3 kg m^{-3}, respectively (Christensen & Mooney 1995). An additional high-velocity lower crustal layer having a *P*-wave velocity of 7.0–7.7 km s^{-1} appears in areas of important tectonic sutures not only beneath Finland, but also in other Precambrian areas (Guggisberg & Berthelsen 1987; Funck *et al.* 2001; Hall *et al.* 2002; Kozlovskaya *et al.* 2002). This additional layer is associated with large Moho offsets and is usually explained as resulting from magmatic intraplating and underplating (Korsman *et al.* 1999; Funck *et al.* 2001; Hall *et al.* 2002).

Our result demonstrates (Fig. 9) that this layer has a density of more than 3.0 $\times$ 10^3 kg m^{-3} that can reach a value of 3.25 $\times$ 10^3 kg m^{-3} at the base of the crust. If this increased density is not taken into consideration, the model contains a mass deficit at the base of the crust and gives rise to a large negative residual anomaly, which is sometimes interpreted as evidence of the anomalous density in the upper mantle. For example, a negative residual anomaly of −50 to −100 mgal was obtained for the Fennoscandian Shield in the

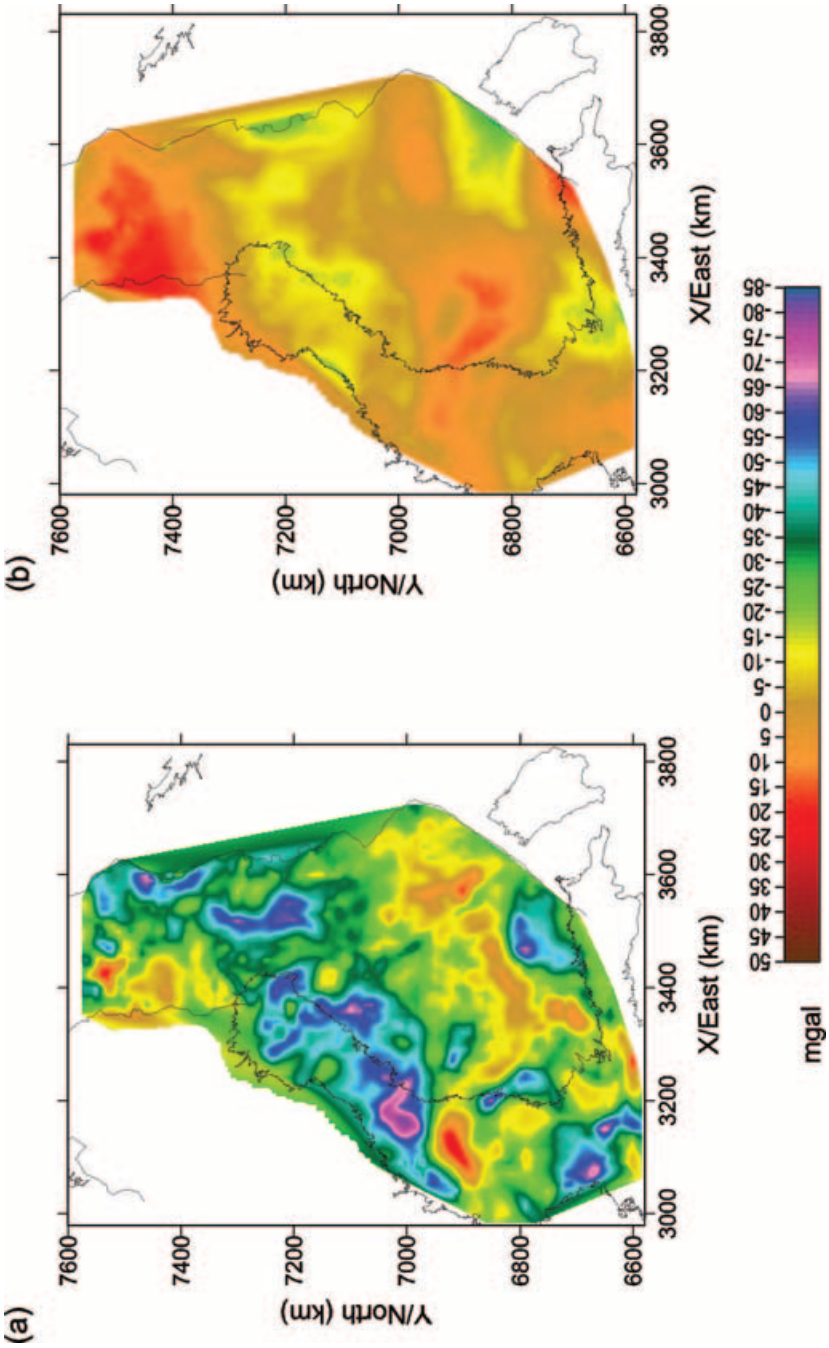

Figure 8. (a) The calculated gravity effect of the crustal density model obtained as a result of gravity data inversion; (b) the residual of the observed Bouguer anomaly and the calculated gravity effect. The values of the gravity field are in units of mgal (10^{-5} m s^{-2}).

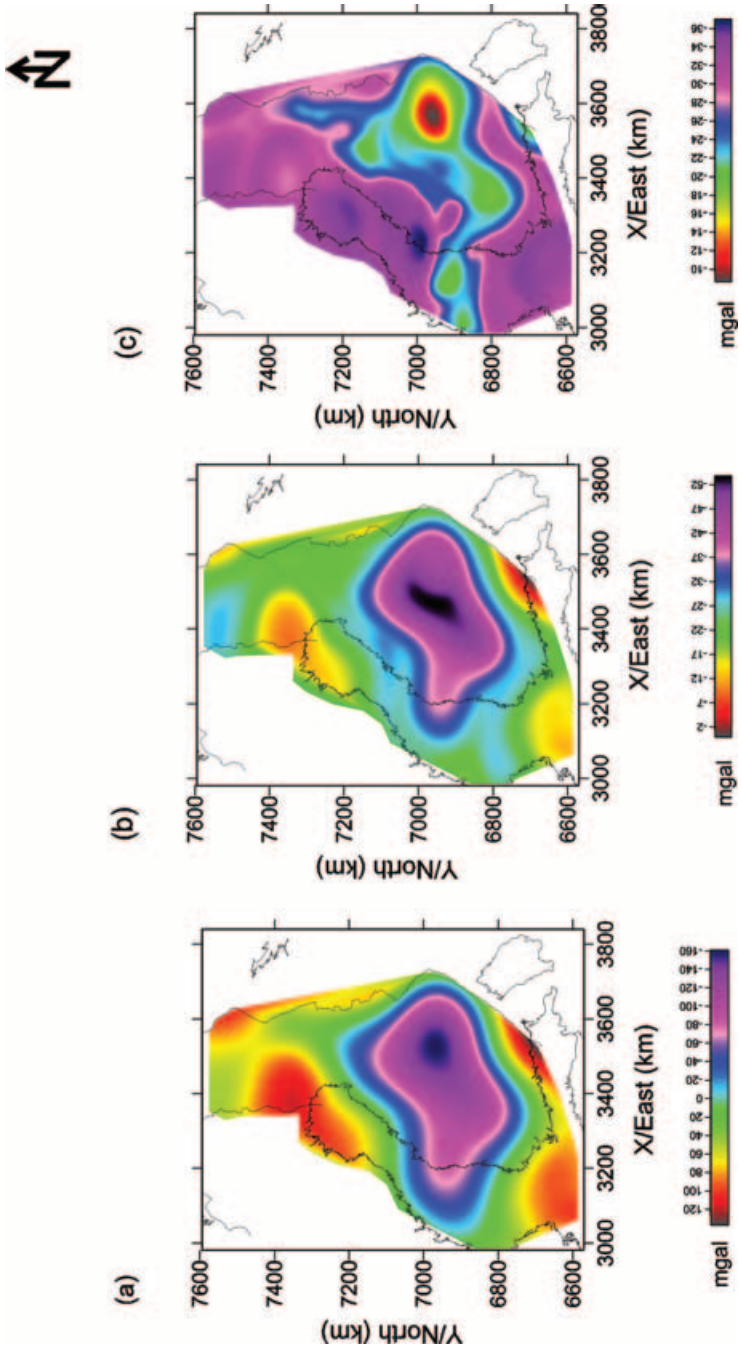

Figure 9. (a) The gravity effect of the crust calculated under the assumption that the density below and above the Moho is constant and equal to 3.35×10^3 and 2.71×10^3 kg m^{-3}, respectively; (b) the gravity effect of the crust calculated under the assumption that the density above the high-velocity lower crustal layer is constant and equal to 2.71×10^3 kg m^{-3}; (c) the gravity effect of the crust calculated under the assumption that the density above the upper/middle crust boundary is constant and equal to 2.71×10^3 kg m^{-3}.

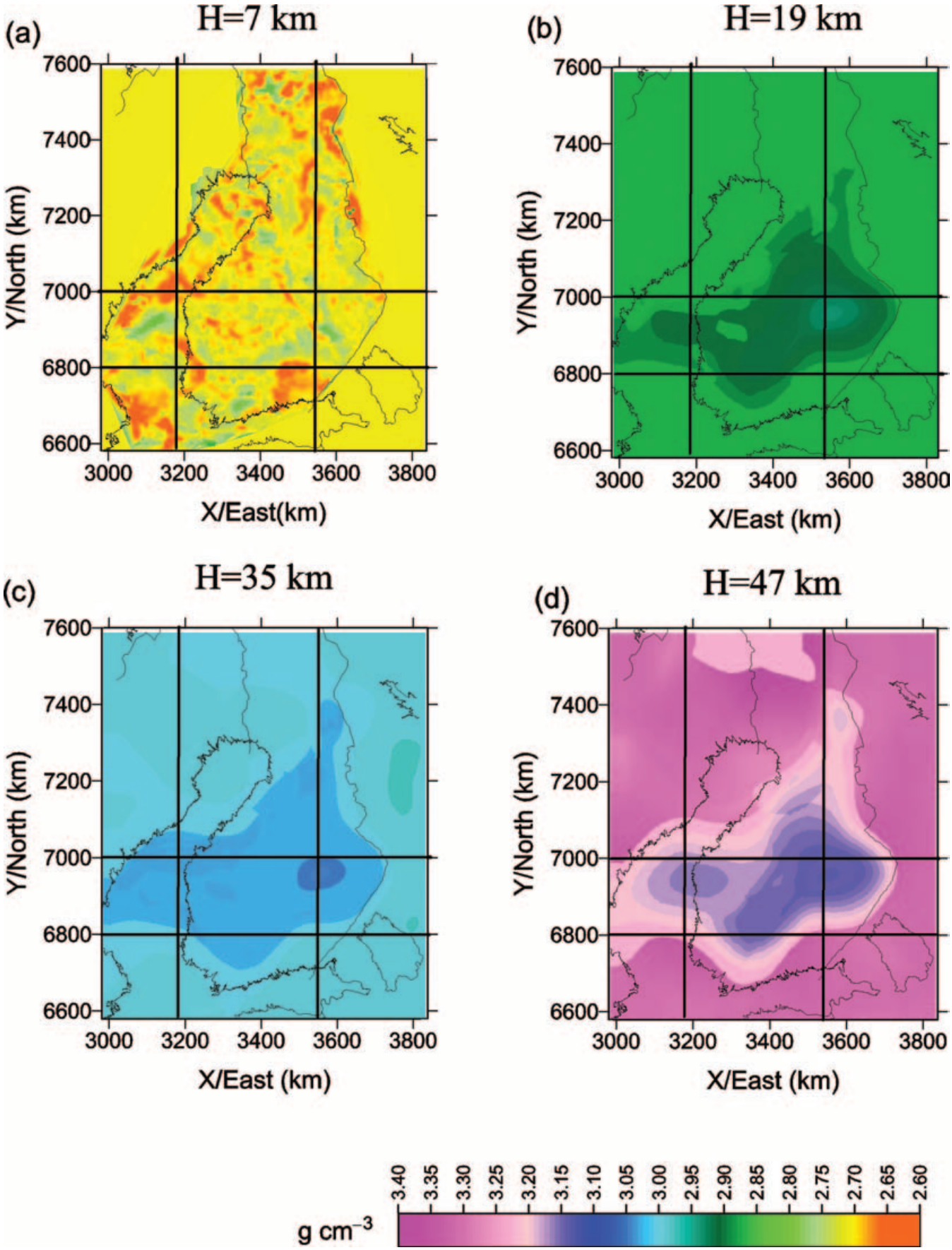

Figure 10. Horizontal cross-sections of the 3-D density model of the SVEKALAPKO area at various depth corresponding to the upper, middle andust and the upper mantle. The values of density are given in units of 10^3 kg m^{-3}. Black bold lines indicate the positions of the four vertical cross-sections shown in Fig. 11.

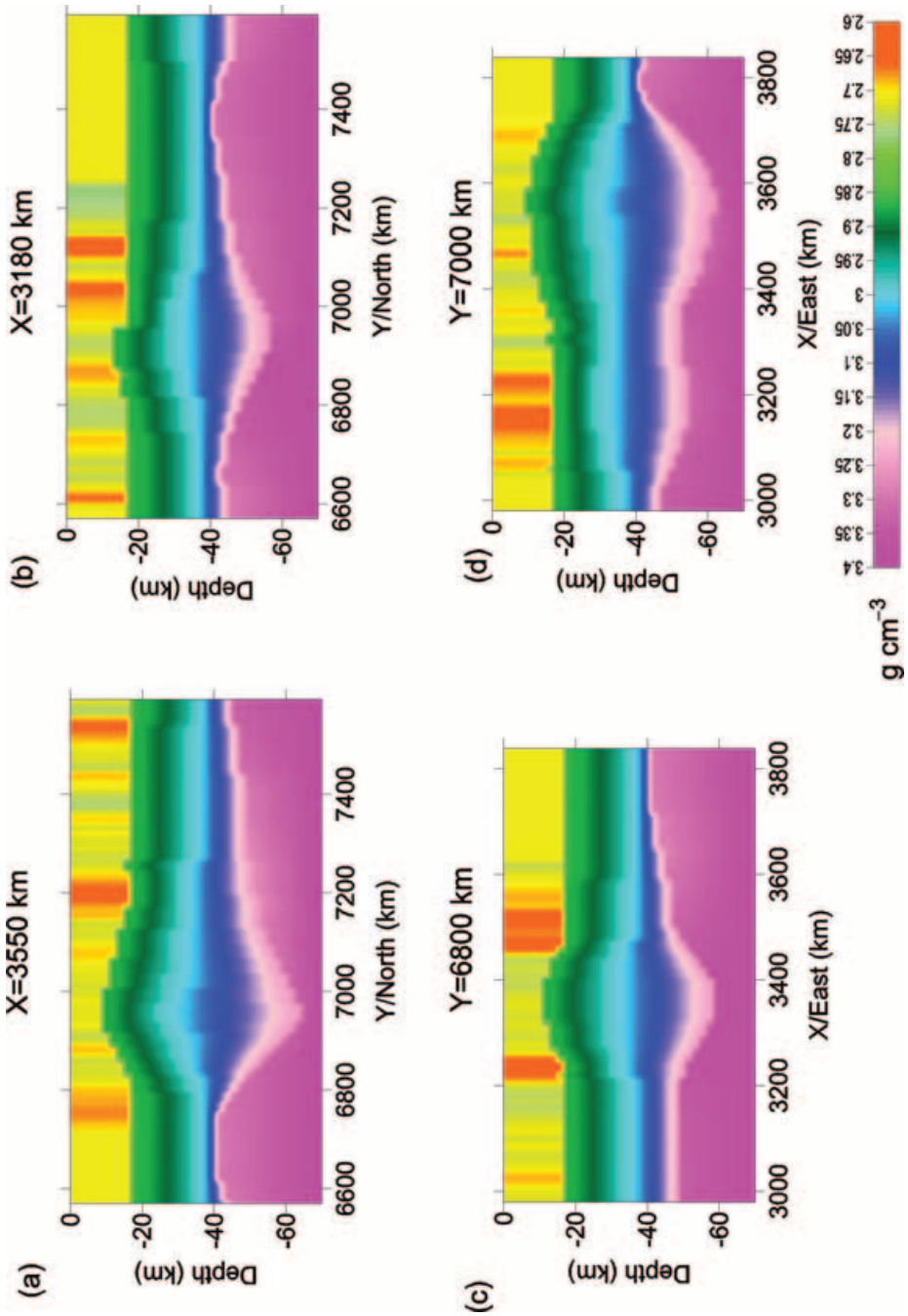

Figure 11. Vertical cross-sections of the 3-D density mode of the SVEKALAPKO area along four profiles. The values of density are given in units of 10^3 kg m $^{-3}$. The location of the profiles is shown in Fig. 10.

recent study by Yegorova & Starostenko (2002), who approximated the crust by vertical blocks with uniform density. Such an approximation resulted in unrealistically small density at the base of the crust beneath the Fennoscandian Shield (2.83–2.9 $\times$ 10^3 kg m^{-3}) and a significant density contrast at the Moho. A residual anomaly of such a large scale does not arise if the increased density of the high-velocity lower crustal layer is taken into consideration. Glaznev *et al.* (1996) and Elo (1997) came to a similar conclusion regarding a high density (3.1–3.2 $\times$ 10^3 kg m^{-3}) in the lower crust above the Moho depression in central Finland. Their models do not give rise to large-scale residual anomalies that can be attributed to significant density variations in the upper mantle.

The example above demonstrates that knowledge of the density of the high-velocity lower crust is very important not only for crustal studies, but for deep lithospheric studies in Precambrian areas as well. To reach any conclusion about the composition of the high-velocity lower crustal layer, the density and velocity values should be compared with the results of laboratory measurements of rock properties and xenolith studies in the region. The reflectivity properties of the crust–mantle boundary revealed by seismic studies are also very important.

Previously, a high-velocity lower crust was revealed along the FENNOLORA profile in Sweden (Guggisberg & Berthelsen 1987). Henkel *et al.* (1990) interpreted the high-velocity lower crust with a velocity and density of 7.1–7.5 km s^{-1} and 3.15–3.27 $\times$ 10^3 kg m^{-3}, respectively, as composed mainly of rocks that have reached transition to eclogite facies. The average depth to this transition was estimated to be at approximately 36.5 km under present pressure and temperature conditions of the shield. This value agrees well with the depth to the high-velocity lower crust estimated by seismic methods and explains the rather flat topography of this boundary.

It should be pointed out, however, that the *P*-wave velocity obtained for the high-velocity lower crust is lower than the *P*-wave velocity of plagioclase-free eclogites estimated from laboratory measurements. The elastic properties of eclogites from different locations have been studied recently by Bascou *et al.* (2001), who determined very high values of *P*-wave velocity and density (8.39–8.75 km s^{-1} and 3.327–3.544 $\times$ 10^3 kg m^{-3}, respectively) for these rocks. Another recent study of the seismic properties of crustal rocks by Kern *et al.* (2002) gave similar values of *P*-wave velocity and density for eclogites. It can be seen that the V_p values for eclogites are generally higher than the values determined by seismic studies for the high-velocity lower crust, even when the effect of pressure and temperature estimated by Christensen & Mooney (1995) is taken into consideration.

The recent results of laboratory investigations of elastic properties of crustal rocks demonstrated that high-pressure mafic garnet granulites have rather high values of velocity and density. These values are similar to those detected in the high-velocity lower crust by seismic studies (Christensen & Mooney 1995). The high-pressure granulites form at pressures comparable to those of eclogite facies but contain plagiolcase and garnet in different proportions. Typically, they are also orthopyroxene-free. O'Brien & Rötzler (2003) pointed out that the high temperatures necessary for formation of high-pressure granulites can be reached in the lower crust as a result of short-lived tectonic events that led to crustal thickening or subduction of the crust into the mantle. Such high-pressure granulites may also represent overprinted eclogites. High-pressure granulites may also form at the crust–mantle boundary as a result of decrease in heat flow in old, thickened continental crust over time, that is, as a result of isobaric cooling from granulite into eclogite facies.

Theoretical calculations of elastic properties of garnet granulite xenoliths from the Archangelsk area (NW Russia; Markwick & Downes 2000) and from the Fennoscandia–Sarmatia junction (SE Belarus; Markwick *et al.* 2001) demonstrated that these rocks have high values of *P*-wave velocity and density under pressures and temperatures corresponding to the depth of the lower crust (6.94–7.7 km s^{-1} and 3.2–3.5 $\times$ 10^3 kg m^{-3}, respectively). The reported V_p values are comparable to the high velocity for the lower crust used in the present study and also to the values derived by the seismic studies beneath the EUROBRIDGE'96 profile (Kozlovskaya *et al.* 2002). The density values obtained from the gravity data interpretation for the high-velocity lower crust are slightly smaller (3.1–3.25 $\times$ 10^3 kg m^{-3}) and are closer to the average density of mafic garnet granulites of 3.15 $\times$ 10^3 kg m^{-3} given by Christensen & Mooney (1995).

The other important constraint on the composition of the high-velocity lower crust in the area is the high reflectivity at the Moho boundary (Grad & Luosto 1987; Luosto *et al.* 1990; BABEL Working Group 1993; Alinaghi *et al.* 2003; Yliniemi *et al.* 2004), which indicates the presence of rocks with contrasting elastic properties at the base of the crust. Deemer & Hurich (1994), Bascou *et al.* (2001) and Kern *et al.* (2002) have demonstrated that the contact of eclogites with the upper-mantle peridotites cannot be the source of strong reflections, while the contact of mafic granulites with the upper-mantle peridotites can. The strong reflections may also result from the contact of eclogite with any other type of crustal rock (Bascou *et al.* 2001). That is why the high-velocity lower crust beneath central and southern Finland is most probably composed of high-pressure garnet granulites, although a certain quantity of eclogite may be present at the base of the crust. This supposition is in agreement with recent studies of xenoliths from the Lahtojoki kimberlite pipe (eastern Finland), which are mainly mafic granulites with varying garnet content (Hölttä *et al.* 2000), although a small quantity of eclogite derived from depths of 150–220 km has also been revealed (Peltonen *et al.* 2002). The values of density at the base of the crust in our model (3.25 $\times$ 10^3 kg m^{-3}) agree with this supposition.

The results of the present study demonstrate that the high-velocity lower crust does not compensate completely the Moho depressions in the area. That is, the compensation is mostly the result of the presence of additional dense material in the upper and middle crust, as was proposed also by Elo (1997) and Korsman *et al.* (1999). As can be concluded from comparison of Fig. 6(d) to Fig. 10, the high density in the upper and middle crust is observed in the places where the Moho depth exceeds 50 km. The different degree of compensation may indicate a different origin and age of the present day Moho that is generally defined by the last major tectonothermal event in the area.

Thus, Moho depressions in central and southern Finland and in the vicinity of the Ladoga–Bothnian Bay zone (LBBZ) are fully compensated, or even overcompensated by dense rocks in the upper and middle crust and hence no corresponding minimum of the Bouguer anomaly is observed. The formation of the thick crust and present-day Moho geometry here was the result of several consecutive tectonic processes during the Svecofennian orogeny between 1885 and 1800 Ga that were concluded by magmatic underplating (Korsman *et al.* 1999). The increased density in the upper and middle crust here resulted from both mafic magmatism and thrusting of highly metamorphosed crust toward the surface.

On the other hand, the Moho depression beneath the Gulf of Bothnia (Figs 10b and 11b) is compensated only in the southern part, where the dense rocks (2.75–2.9 $\times$ 10^3 kg m^{-3}) are located in the middle and upper crust. The density in the upper and middle

crust in the northern part of the depression is significantly less (2.6–2.85 $\times$ 10^3 kg m^{-3}), which results in a large regional-scale Bouguer anomaly low (Figs 2a and 8a). The low values of density in the upper crust here can be explained by the combined effect of sediments and granitic rocks, although these have very similar values of density (Elo *et al.* 1978) and cannot be separated from each other in our model.

The thick crust beneath the Gulf of Bothnia was considered to be part of the Svecofennian orogen (1.92–1.8 Ga) and is believed to have been intruded by anorogenic rapakivi granites and gabbro–anorthosites during 1.58–1.53 Ga (Korja *et al.* 2001). The latest magmatic event is associated with post-Jotnian diabase dykes and sills emplaced between 1.1–1.2 Ga (Kohonen & Rämö 2002). According to Korja *et al.* (2001), two different types of magmatic rocks, the rapakivi granites in the northern part and the gabbro–anorthosites in the southern part of the Moho depression in the Gulf of Bothnia, may explain the variation of upper and middle crustal density. However, the connection between intensive magmatic processes and the present-day geometry of the lower crust and Moho is not completely clear in this case, because the other known areas of intensive bimodal magmatism in the region are characterized by uplift of the Moho instead of depression, as observed beneath the Wyborg rapakivi batholith (Elo & Korja 1993).

The tectonic model of the Svecofennian orogen has been revised recently by Lahtinen *et al.* (2004), who suggested that the Svecofennian domain was formed as a result of five different orogenic processes in the time period 1.92–1.88 Ga and that the whole Fennoscandian segment of the lithosphere was formed as a result of the accretion of several microcontinents. Although not all aspects of the new model are completely clear, we may suppose that the two crustal blocks with different density and *P*-wave velocity may correspond to two accreted microcontinents (or terranes?) proposed by the authors. This suggestion explains not only different values of V_p and density of the crust in the northern and southern parts of the Moho depression, but also the origin of the deep Moho in this place.

10 CONCLUSIONS

A 3-D regional density model has been compiled for the crust of southern and central Finland, where the thickness of the crust varies from 38 to 64 km. The model agrees well with the observed Bouguer anomaly and explains the sources of large-scale Bouguer anomalies in the region.

The main features of density distribution within the crust are not correlated with the variations in depth. However, the large-scale Moho depressions in the region mark the boundaries of crustal blocks with different styles of density distribution within the crust and are associated with the presence of additional compensating masses in the crust.

The high-velocity lower crust, having a density of 3.1–3.25 $\times$ 10^3 kg m^{-3}, compensates for a significant part of the gravity effect produced by the variations in the crustal thickness in the area. The rest of this effect is compensated by a distribution of masses in the upper and middle crust. Overcompensation or undercompensation results in large maxima or minima of the gravity field, respectively.

Thus, the Moho depressions in central and southern Finland are fully compensated, or even overcompensated by dense mafic rocks. On the other hand, the Moho depression in the area of the Gulf of Bothnia is compensated only in its southern part, resulting in a regional-scale minimum of the Bouguer anomaly in the northern part of the depression. The differing degrees of compensation may result from varying origin and age of the Moho boundary and the crust in the region.

The model presented here explains only regional trends in the observed Bouguer anomaly. A further study of selected anomalies is necessary to give a more detailed picture of the density distribution within the crust beneath the SVEKALAPKO area.

ACKNOWLEDGMENTS

The present work is a joint effort of the EUROPROBE/SVEKALAPKO multididisciplinary project (SVEKALAPKO/Integrated interpretation and 3-D Crustal Model of the SVEKALAPKO research area), financed by the Academy of Finland and the Crustal Model Program for Finland carried out by the Geological Survey of Finland. The gravity maps used in our study were compiled by J. Korhonen from original data acquired by the Geological Survey of Finland and the Finnish Geodetic Institute. Calculations of the gravity field and inversions were performed on the SGI Origin 2000 parallel computer at the Finnish Center for Scientific Computing (CSC-Scientific Computing Ltd.).

The authors appreciate very much the help of Professor E. Kissling and Dr S. Sandoval, who provided the crustal V_p velocity model for the present investigation. The authors are very grateful to Dr M. Ollikainen of the Finnish Geodetic Institute for the computer codes for coordinate transformation. The help of Dr T. Korja from the Department of Geophysics of Oulu University, who provided a simplified geological map of the area, is highly appreciated. The authors thank the two journal reviewers, Mr Paul Williamson and Dr H. Henkel, for their helpful comments and suggestions for improving the manuscript.

REFERENCES

Alinaghi, A., Bock, G., Kind, R., Hanka, W., Wylegalla, K., TOR & SVEKALAPKO Working Groups. 2003. Receiver function analysis of the crust and upper mantle from the North German Basin to the Archaean Baltic Shield, *Geophys. J. Int.,* **155,** 641–652.

BABEL Working Group, 1993. Integrated seismic studies of the Baltic Shield using data in the Gulf of Bothnia region, *Geophys. J. Int.,* **112,** 305–324.

Banerjee, B. & Das Gupta, S.P., 1977. Gravitational attraction of rectangular parallelepiped, *Geophysics,* **42**(5), 1053–1055.

Bascou, J., Barruol, G., Vauches, A., Mainprice, D. & Egylio-Silva, M., 2001. EBSD-measured lattice-preferred orientation and seismic properties of eclogites, *Tectonophysics,* **342,** 61–80.

Berzin, R.G., Yurov, Yu.G. & Pavlenkova, N.I., 2002. CDP and DSS data along the Uchta-Kem profile (the Baltic Shield), *Tectonophysics,* **355,** 187–200.

Birch, F., 1961. The velocity of compressional waves in rocks to 10 kilobars (Part II), *J. geophys. Res.,* **65,** 1083–1102.

Bock, G. (ed.) & SVEKALAPKO Seismic Tomography Working Group, 2001. Seismic probing of Archaean and Proterozoic Lithosphere in Fennoscandia, *EOS, Trans. Am. geophys. Un.,* **82**(50), 621, 628–629.

Christensen, N.I. & Mooney, W.D., 1995. Seismic velocity and composition of the continental crust: a global view, *J. geophys. Res.,* **100,** 9761–9788.

Deemer, S.J. & Hurich, C.A., 1994. The reflectivity of magmatic underplating using the layered mafic intrusion analog, *Tectonophysics,* **232,** 239–255.

Elo, S., 1997. Interpretation of the Gravity Anomaly Map of Finland, *Geophysica,* **33**(1), 51–80.

Elo, S. & Korja, A., 1993. Geophysical interpretation of the crustal and upper mantle structure in the Wiborg rapakivi gravity area, southeastern Finland, *Precambrian Research,* **64,** 273–288.

Elo, S., Puranen, R. & Airo, M., 1978. Geological and areal variation of rock densities, and their relation to some gravity anomalies in Finland, *GeoScrifter,* **10,** 123–164.

Funck, T., Louden, K.E. & Reid, I.D., 2001. Crustal structure of the Grenville Province in Southeastern Labrador from refraction seismic data—evidence for a high-velocity lower crustal wedge, *Can. J. Earth Sci.,* **38,** 1463–1478.

Ganchin, Y.V., Smithson, S.B., Morozov, I.B., Smythe, D.K., Garipov, V.Z., Karaev, N.A. & Kristofferson, Y., 1998. Seismic studies around the Kola Superdeep Borehole, Russia, *Tectonophysics,* **288,** 1–16.

Glaznev, V.N., Raevsky, A.B. & Skopenko, G.B., 1996. A three dimensional integrated density and thermal model of the Fennoscandian Lithosphere, *Tectonophysics,* **258,** 15–33.

Goff, J.A. & Holliger, K., 1999. Nature and origin of upper crustal seismic velocity fluctuations ans associated scaling properties: combined stochastic analyses of KTB velocity and lithology logs, *J. geophys. Res.,* **104,** 13 169–13 182.

Grad, M. & Luosto, U., 1987. Seismic models of the crust of Baltic Shield along the SVEKA profile in Finland, *Ann. Geophys.,* **5B,** 639–650.

Graham, D.P., Matthews, P.A. & Long, R.E., 1992. Interpretation of wide angle and normal incidence reflection data from BABEL line 1, in *The BABEL Project. First Status Report. Commission of the European Communities,* pp. 93–96, eds Meissner, R., Snyder, D., Balling, N., Staroste, E., Directorate-General Science, Research and Development, Brussels.

Green, D.H. & Ringwood, A.E., 1967. An experimental investigation of the gabbro to eclogite transformation and its petrological applications, *Geochim. cosmochim. Acta,* **31,** 767–833.

Guggisberg, B. & Berthelsen, A., 1987. A two-dimensional velocity model for the lithosphere beneath the Baltic Shield and its possible tectonic significance, *Terra Cognita,* **7,** 631–638.

Gutscher, M.-A., 1995. Crustal structure and dynamics in the Rhine Graben and the Alpine foreland, *Geophys. J. Int.,* **122,** 617–636.

Hall, J., Louden, K.E., Funck, T. & Deemer, S., 2002. Geophysical characteristics of the continental crust along the LITHOPROBE Eastern Canadian Shield Onshore-Offshore Transect (ECSOOT): a review, *Can. J. Earth Sci.,* **39,** 569–587.

Heikkinen, P. & Luosto, U., 2000. Review of some features of the seismic velocity models in Finland. In: *LITHOSPHERE 2000. A Symposium on the Structure, Composition and Evolution of the Lithosphere in Finland* (eds Pesonen, L., Korja, A. & Hjelt, S.-E.), pp. 35–41, Extended Abstracts 4–5.10.2000, GSF, Espoo.

Henkel, H., Lee, M.K. & Lund, C.-E., 1990. An integrated geophysical interpretation of the 2000 km FENNOLORA section of the Baltic Shield, in *The European Geotraverse: Integrative studies,* pp. 1–48, eds Freeman, R., Giese, P. & Mueller, St., ESF, Strasbourg, France.

Hirvonen, R.A., 1949. Die Gauss-Krügerische Projektion für breite Meridianstreifen auf dem Internationalen Ellipsoide. Suomen Geodeettisen laitoksen julkaisuja, 36, Helsinki.

Hjelt, S.-E., 1974. The gravity anomaly of a dipping prism, *Geoexploration,* **12,** 29–39.

Hjelt, S.-E., Daly, S. & SVEKALAPKO colleagues, 1996. SVEKALAPKO. Evolution of Palaeoproterozoic and Archaean Lithosphere, in *EUROPROBE 1996—Lithospheric Dynamics: Origin and Evolution of Continents,* pp. 56–67, eds Gee, D.G. & Zeyen, H.J., EUROPROBE Secretariate, Uppsala University, Uppsala.

Hoffmann, Y., Jahr, T. & Jentsch, G., 2003. Three-dimensional gravimetric modelling to detect the deep structure of the region Vogtland/NW-Bohemia, *J. Geodyn.,* **35,** 209–220.

Hölttä, P., Huhma, H., Mänttäri, I., Peltonen, P. & Juhanoja, J., 2000. Petrology and geochemistry of mafic granulite xenoliths from the Lahtojoki kimberlite pipe, eastern Finland, *Lithos,* **51,** 109–133.

Jones, A.G. & Holliger, K., 1997. Spectral analysis of the KTB sonic and density logs using robust nonparametric methods, *J. geophys. Res.,* **102,** 18 391–18 403.

Kääriäinen, J. & Mäkinen, J., 1997. The 1979-1996 gravity survey and results of the gravity survey of Finland, *Publications of the Finnish Geodetic Institute,* **125,** 47–56.

Kern, H. & Richter, A., 1981. Temperature derivates of compressional and shear wave velocities in crustal and mantle rocks at 6 kbar confining pressure, *J. Geophys.,* **49,** 47–57.

Kern, H., Walther, Ch., Flüh, E.R. & Marker, M., 1993. Seismic properties of rocks exposed in the POLAR profile region—constraints on the interpretation of the refraction data, *Precambrian Research,* **64,** 169–187.

Kern, H., Jin, J., Gao, S., Popp, T. & Xu, Z., 2002. Physical properties of ultrahigh-pressure metamorphic rocks from the Sulu terrain, eastern central China: implications for the seismic structure at the Dongai (CCSD) drilling site, *Tectonophysics,* **354,** 315–330.

Klaeshen, D. & Flueh, E.R., 1996. Reprocessing of BABEL line 1 normal incidence data, in *The BABEL Project, Final Status Report, EUR 16486,* pp. 77–85, eds Meissner, R.R. *et al.,* European Commission, Directorate-General, Science, Research and Development, Brussels.

Kneib, G., 1995. The statistical nature of the upper continental crystalline crust derived from in situ seismic measurements, *Geophys. J. Int.,* **122,** 594–616.

Kohonen, J. & Rämö, T., 2002. Sedimentary record and magmatic episodes reflecting Mezoproterozoic-Phanerozoic evolution of the Fennoscandian Shield. In: *Lithosphere 2002. Second Symposium on the Structure, Composition and Evolution of the Lithosphere in Finland*, eds Lahtinen, R. *et al.*, pp. 23–31, Extended Abstracts 12–13.11.2000, GSF, Espoo.

Korhonen, J., Säävuori, H. & Kivekäs, L., 1997. Petrophysics in the crustal model program of Finland, in, *Geological Survey of Finland,* Vol. 23, Current Research 1995–1996, Special Paper, pp. 157–173, ed. Autio, S., GSF, Espoo.

Korhonen, J.V. *et al.,* 2002. *Bouguer Anomaly Map of the Fennoscandian Shield 1 : 2 000 000,* Geological Surveys of Finland, Norway and Sweden and Ministry of Natural Resources of Russian Federation.

Korja, A., Korja, T., Luosto, U. & Heikkinen, P., 1993. Seismic and geoelectric evidence for collisional and extensional events in the Fennoscandian Shield- implications for Precambrian crustal evolution, *Tectonophysics,* **219,** 129–152.

Korja, T. & the BEAR Working Group., 2000. The structure of the crust and upper mantle in Fennoscandia as imaged by electromagnetic waves. In: *Lithosphere 2000, a Symposium on the Structure, Composition and Evolution of the Lithosphere in Finland,* eds Pesonen, L.J., Korja, A. & Hjelt, S.-E., Report S-41, pp. 25–34, Programme and Extended Abstacts October 4–5, 2000, Inst. Seismology, Univ. Helsinki, Espoo.

Korja, A., Heikkinen, P. & Aaro, S., 2001. Crustal structure of the northern Baltic Sea palaeorift, *Tectonophysics,* **331,** 341–358.

Korsman, K., Korja, T., Pajunen, M., Virransalo, P. & GGT/SVEKA Working Group., 1999. The GGT/SVEKA Transect: Structure and evolution of the continental crust in the Paleoproterozoic Svekofennian Orogen in Finland, *International Geology Review,* **41,** 287–333.

Kozlovskaya, E., 2000. An algorithm of geophysical data inversion based on non-probabilistic presentation of a-priori information and definition of Pareto-optimality, *Inverse Problems,* **16,** 839–861.

Kozlovskaya, E. & Yliniemi, J., 1999. Deep structure of the Earth's crust along the SVEKA profile and its extention to the north-east, *Geophysica,* **1–2,** 111–123.

Kozlovskaya, E., Karatayev, G. & Yliniemi, J., 2001a. Lithosphere structure along the northern part of EUROBRIDGE in Lithuania; results from integrated interpretation of DSS and gravity data, *Tectonophysics,* **339,** 177–191.

Kozlovskaya, E., Yliniemi, J., Karatayev, G. & EUROBRIDGE Seismic Working Group, 2001b. Integrated density–velocity modeling along EUROBRIDGE'95-97 wide-angle reflection and refraction profiles: main results. EUGXI, *Journal of Conference Abstracts,* **6,** 365.

Kozlovskaya, E., Taran, L., Yliniemi, J. & Karatayev, G., 2002. Deep structure of the crust along the Fennoscandia-Sarmatia Junction zone (central Belarus): results of a geophysical-geological integration, *Tectonophysics,* **358,** 97–120.

Krasovsky, S.S., 1981. *Reflection of continental-type crustal dynamics in the gravity field,* Navukova Dumka, Kiev (in Russian).

Lahtinen, R., Korja, A. & Nironen, M., 2004. Palaeoproterozoic tectonic evolution of the Fennoscandian Shield—a plate tectonic model, in *Precambrian Geology in Finland,* ed. Lehtinen, M., Elsevier, Amsterdam.

Lebedev, T.S., 1985. Problems of thermobarometric investigations of the physical properties of lithospheric rocks, *Geofizicheskij Zhurnal,* **7**(6), 62–79 (in Russian).

Lebedev, T.S., Shapoval, V.I. & Korchin, V.A., 1972. New data on longitudinal wave velocities in rocks at high thermodynamic parameters, *Geofizicheskij sbornik,* **49,** 9–27 (in Russian).

Lebedev, T.S., Korchin, V.A. & Burtny, P.A., 1983. Elastic wave velocity in ultrabasic and magmatic rocks under high pressure and temperature and their variation with depth, *Geofizicheskij Zhurnal,* **5**(5), 36–45 (in Russian).

Lebedev, T.S., Novik, G.Y., Korchin, V.A., Zilberschmit, M.G. & Zavorykina, T.K., 1986. The influence of structural transformations of rocks on their elastic properties under various thermobarometric conditions, *Geofizicheskij Zhurnal,* **4**(8), 9–20 (in Russian).

Luosto, U., 1991. Moho depth map of the Fennoscandian Shield based on seismic refraction data, in *Structure and Dynamics of the Fennoscandian Lithosphere,* Rep. S-25, pp. 43–49, eds Korhonen, H. & Lipponen, A., Inst. Seism., Univ. Helsinki, Helsinki.

Luosto, U., 1997. Structure of the Earth's crust in Fennoscandia as revealed from refraction and wide-angle reflection studies, *Geophysica,* **33**(1), 3–16.

Luosto, U., Lanne, E., Korhonen, H., Guterch, A., Grad, M., Materzok, R. & Perchuc, E., 1984. Deep structure of the Earth's crust on the SVEKA profile in central Finland, *Annales Geophysicae,* **2,** 559–570.

Luosto, U. *et al.,* 1990. Crust and upper mantle structure along the DSS BALTIC profile in SE Finland, *Geophys. J. Int.,* **101,** 89–110.

Markwick, A.J.W. & Downes, H., 2000. Lower crustal granulite xenoliths from the Archangelsk kimberlite pipes: petrophysical, geochemical and geophysical results, *Lithos,* **51,** 135–151.

Markwick, A.J.W., Downes, H. & Veretennikov, N., 2001. The lower crust of SE Belarus: petrological, geophysical and geochemical constraints from xenoliths, *Tectonophysics,* **339,** 215–237.

Meissner, R. & Rabbel, W., 1999. Nature of crustal reflectivity along the DEKORP profiles in Germany in comparison with reflection patterns from different tectonic units worldwide: a review, *Pure appl. Geophys.,* **156,** 7–28.

Mudretsova, E.A. & Veselov, K.E. (eds), 1990. *Gravity exploration: a handbook of a geophysicist,* Nedra, Moscow (in Russian).

Nafe, J.E. & Drake, C.L., 1957. Variation with depth in shallow and deep water marine sediments of porosity, density and the velocities of compressional and shear waves, *Geophysics,* **22,** 523–552.

Nagy, D., 1966. The gravitational attraction of a right rectangular prism, *Geophysics,* **31,** 362–371.

Nielsen, L., Balling, N., Jacobsen, B.H. & MONA LISA Working Group., 2000. Seismic and gravity modeling of crustal structure in the Central Graben, North Sea. Observations along MONA LISA profile 3, *Tectonophysics,* **328,** 229–244.

O'Brien, P.J. & Rötzler, J., 2003. High-pressure granulites: formation, recovery of peak conditions and implications for tectonics, *J. metamorphic Geol.,* **21,** 3–20.

Ollikainen, M., Koivula, H. & Poutanen, M., 2001. *EUREF-FIN—koordinaatisto ja EUREF-pistetihennykset Suomessa,* Tiedote 24, Geod. Laitos, Massala (in Finnish).

Pavlenkova, N.I., Luosto, U., Yliniemi, J. & Ansorge, J., 2001. 3-D P-velocity model of the crust in the Baltic Shield. In: *6th SVEKALAPKO Workshop, 29.11–2.12.2001* p. 43, ed. Hjelt, S.-E., Lammi, Finland.

Peltonen, P., Kinnunen, K.A. & Huhma, H., 2002. Petrology of two diamondiferous eclogite xenoliths from the Lahtojoki kimberlite pipe, eastern Finland, *Lithos,* **63,** 151–164.

Rasmussen, R. & Pedersen, L.B., 1979. End corrections in potential field modelling, *Geophys. Prospect.,* **27,** 749–760.

Ruotoistenmäki, T., 1994a. The gravity anomaly of three-dimensional sources characterized by arbitrary surfaces and density distributions, *J. appl. Geophys.,* **32,** 177–186.

Ruotoistenmäki, T., 1994b. Calculation of gravity anomalies of 3D sources using drillhole density data, *J. appl. Geophys.,* **36,** 131–136.

Sandoval, S., 2002. The lithosphere-asthenosphere system beneath Fennoscandia (Baltic Shield) by body-wave tomography, *PhD thesis*, No. 14 689. Swiss Federal Institute of Technology. Zürich.

Sandoval, S., Kissling, E., Ansorge, J. & the SVEKALAPKO STWG, 2003. High-Resolution body wave tomography beneath the SVEKALAPKO array: I. A-priori 3D crustal model and associated traveltime effects on teleseismic wavefronts, *Geophys. J. Int.,* **153,** 75–87.

Schön, J.H., 1998. *Physical properties of rocks: fundamental and principles of petrophysics,* Pergamon, the Netherlands.

Smithson, S.B., Wenzel, F., Ganchin, Y.V. & Morozov, I.B., 2000. Seismic results at Kola and KTB deep scientific boreholes: velocities, reflections, fluids, and crustal composition, *Tectonophysics,* **329,** 301–317.

Sobolev, S.V. & Babeyko, A.Y., 1994. Modeling of mineralogical composition, density and elastic wave velocities in anhydrous magmatic rocks, *Surv. Geophys.,* **15,** 515–544.

Spear, F.S., 1993. *Metamorphic phase equilibra and pressure-temperature-time paths,* Mineralogical Society of America, Washington, DC.

Starostenko, V.I., 1998. The gravity field of polygonal plates and related prisms: a review. Izvestiya, *Physics of the solid Earth,* **34**(3), 209–224.

Thybo, H. *et al.,* 2003. Upper lithospheric seismic velocity structure across the Pripyat Trough and the Ukrainian Shield along the EUROBRIDGE'97 profile, *Tectonophysics,* **371,** 41–79.

Wang, Z., 1998. *Geoid and crustal structure in Fennoscandia,* Report 126, Finn. Geod. Inst., Kirkkonummi.

White, D.J., 1996. Reprocessing of seismic reflection data from BABEL Line 1, in *The BABEL Project, Final Status Report, EUR 16486,* pp. 77–85, eds Meissner, R.R. *et al.,* European Commission, Directorate-General, Science, Research and Development, Brussels.

Yegorova, T.P. & Starostenko, V.I., 2002. Lithosphere structure of Europe and Northern Atlantic from regional three-dimensional gravity modelling, *Geophys. J. Int.,* **151,** 11–31.

Yliniemi, J., 1991. Deep seismic soundings in the University of Oulu. In:, *Structure and dynamics of the Fennoscandian lithosphere. Proceedings of the 2nd Workshop on investigation of the lithosphere in the Fennoscandian Shield by seismological methods, May 14–18* (eds Korhonen, H. & Lipponen, A.), pp. 1–6, University of Helsinki, Helsinki.

Yliniemi, J., Jokinen, J. & Luukkonen, E., 1996. Deep structure of the Earth's crust along the GGT/SVEKA transect extension to northeast. In: *Global Geoscience Transect/SVEKA. Proceedings of the Kuopio seminar, Finland 25-26/11/1993,* eds Ekdahl, E. & Autio, S., Geological Survey of Finland, Espoo.

Yliniemi, J., Kozlovskaya, E., Hjelt, S.-E., Komminaho, K., Ushakov, A. & SVEKALAPKO Seismic Tomography Working Group., 2004. Structure of the crust and uppermost mantle beneath southern Finland revealed by analysis of local events registered by the SVEKALAPKO seismic array, *Tectonophysics,* submitted.

APPENDIX A: FAST CALCULATION OF THE GRAVITY EFFECT OF LARGE-SCALE 3-D DENSITY MODELS

It is well known that the 3-D distribution of mass within the Earth is rather complex. As there exists no analytical solution for the gravity potential of an arbitrary complex earth model, its gravity effect is often modelled as a superposition of the gravity effects of a limited number of simple bodies, for which the analytical expressions for the gravity potential and its derivatives are known. The most widely used class of such elementary gravity sources are polygonal prisms of various kinds, as the analytical expressions for gravity anomalies produced by them are widely known from literature (Nagy 1966; Hjelt 1974; Banerjee & Das Gupta 1977; Ruotoistenmäki 1994a,b; Starostenko 1998). Use of these expressions requires numerical calculation of non-linear functions such as arctan and logarithm. The problem is that in order to represent adequately realistic 3-D density distributions by elementary prismatic bodies, a number of them are required to be large enough and this results in a significant increase of computer time. A second problem is connected with the use of absolute density values, which gives rise to a large positive offset in

the calculated gravity as well as side effects. To avoid these problems, we approximate the density model with a fine grid embedded in a layered model. This makes it possible to use the simpler expression for an elementary mass instead of that for a prism and to treat edge effects simultaneously.

A1 Discretization of the density model

The first derivative of the gravitational potential caused by an arbitrary density distribution $\rho\ (x, y, z)$ within a finite volume T at an observation point $P = (x_0, y_0, z_0)$ can be calculated in the Cartesian coordinate system as:

$$V_z(x_0, y_0, z_0) = G \int_T \frac{\rho(x, y, z)(z - z_0)}{r^3} dT, \tag{A1}$$

where $r = \sqrt{(x - x_0)^2 + (y - y_0)^2 + (z - z_0)^2}$, G is the gravitational constant and $dT = dx\,dy\,dz$ is an elementary mass volume. The second derivative of the gravitational potential of an elementary mass at the point $(x_0\ , y_0, z_0)$ is therefore

$$V_z(x_0, y_0, z_0) = G \frac{\rho(x, y, z)(z - z_0)\,dx\,dy\,dz}{r^3}. \tag{A2}$$

If the density distribution within the volume T is parametrized by a fine regular grid, i.e. $dx = dy = dz$, the density in each elementary volume (cell) can be assumed to be constant and attributed to the centre of the cell. Then the integral eq. (A1) can be calculated by summation of gravity effects of all cells:

$$V_z(x_0, y_0, z_0) = GdT \sum_{i=1}^{nx} \sum_{j=1}^{ny} \sum_{k=1}^{nz} \frac{\rho_{ijk}(k\Delta z - z_0)}{R^3},$$
$$R = \sqrt{(i\Delta x - x_0)^2 + (j\Delta y - y_0)^2 + (k\Delta z - z_0)^2}. \tag{A3}$$

Eq. (A3) will provide good accuracy of the calculated gravity effect if the sizes of the elementary cells are significantly less than the size of the model, that is, $nx \gg 1$, $ny \gg 1$, $nz \gg 1$ and the grid spacing is several times less than the distance between observation points. However, its use requires that the gravity effect of an elementary cell described by eq. (A2) is calculated $nx \times ny \times nz$ times for each observation point. Thus, if the number of observation points is $nx \times ny$, then the total number of calculations of the expression of eq. (A2) is $nx^2 \times ny^2 \times nz$. Such a large amount of calculations can be treated using parallelization of the computer code, which can be easily done by distribution of calculation of the gravity effect of separate cells between several processing units.

The total amount of computer time for calculation of eq. (A3) can be significantly decreased, if the symmetry of the gravity effect produced by a point mass is taken into consideration. Specifically, the gravity effect of the point mass in eq. (A2) depends only on the depth from the surface, the value of density at this point and the distance from the observation point. Consequently, it is possible to calculate separately the gravity effect of a unit point mass located at the depth of $k\Delta z$, $k = 1, nz$ at distances varying from zero to the longest distance from a point mass to an observation point in the model, with spacing equal to Δx. The total amount of calculations of eq. (A2) required for this is $nz \times N_d$, where $N_d = \sqrt{nx^2 + ny^2}$. The calculated effects can be stored in an $nz \times N_d$ matrix. Then the gravity effect of each point mass in eq. (A3) can be calculated by multiplying the density value in each node of the grid to the corresponding gravity effects of the unit mass located at the same depth and having the same distance to the observation point. The gravity effect can be extracted directly from the matrix, or found by linear interpolation.

A2 Absolute density values and edge effects

Use of seismic velocity models in gravity data interpretation implies that density may be calculated from the known velocity distribution in accordance with some known density–velocity relationship (for example, Birch 1961; Krasovsky 1981; Christensen & Mooney 1995). Alternatively, the density–velocity relationship can be found as a result of gravity data inversion (Kozlovskaya *et al.* 2001a). This requires that absolute values of densities are used in the gravity field calculations instead of the density contrast conventionally used in the gravity field studies. As a result, the calculated gravity effect of the finite volume T has a large positive offset at the edges of the model. This problem can be avoided by continuing the model to infinity in x and y directions (Rasmussen & Pedersen 1979).

Suppose that we have a density model defined on a regular 3-D grid, in which the numbers of elementary cells in the x, y and z direction are nx, ny and nz, respectively. The model can be continued to infinity by introducing nz layers of constant density equal to the average value of density in each layer:

$$\rho_k = \frac{1}{nxny} \sum_{i=1}^{nx} \sum_{j=1}^{ny} \rho_{ijk}, \quad k = 1, nz. \tag{A4}$$

The density in each cell can be presented as a sum of the density of the host layer and the difference between the density of the host layer and the absolute value of density in this cell:

$$\Delta\rho_{ijk} = \rho_k - \rho_{ijk}, \quad \rho_{ijk} = \rho_k + \Delta\rho_{ijk}, \quad i = 1, nx, j = 1, ny,$$
$$k = 1, nz. \tag{A5}$$

Then the total effect of the density model can be expressed as a sum of the effect of a 1-D density model composed of infinite layers of constant density and a residual 3-D density model composed of cells with densities equal to the differences between the value of density in the cell and the density of the host layer. The gravity effect of an infinite layer with a constant density can be calculated as given by Mudretsova & Veselov (1990).

$$V_z^k(x_0, y_0, z_0) = 2G\pi\rho_k\Delta z. \tag{A6}$$

The gravity effect of the residual 3-D density model is calculated by substituting the residual density values $\Delta\rho_{ijk}$ into eq. (A3).

Although the gravity effect calculated using eqs (A3)–(A6) has no edge effects, it still has a positive offset as a result of the use of absolute density values. For comparison with the observed Bouguer anomaly $\Delta g(x_0\ , y_0\ , z_0)$, the calculated values should be referred to the same average value by adding the residual between the average of the calculated gravity effect and the average of the observed Bouguer anomaly:

$$V_z^{\text{calc}}(x_0, y_0, z_0) = \sum_{i=1}^{k} V_z^k(x_0, y_0, z_0) + GdT \sum_{i=1}^{nx} \sum_{j=1}^{ny} \sum_{k=1}^{nz} \frac{\Delta\rho_{ijk}(k\Delta z - z_0)}{R^3},$$
$$V_z^{\text{total}}(x_0, y_0, z_0) = V_z^{\text{calc}}(x_0, y_0, z_0) - \text{average}\left[V_z^{\text{calc}}(x_0, y_0, z_0)\right] + \text{average}\left[\Delta g(x_0, y_0, z_0)\right]. \tag{A7}$$

This residual represents correction of the calculated gravity effect by the unknown regional trend.